Unravelling the wind impact of clusters of storms, a case study over the French insurer Generali

Laura Hasbini[1,2], Pascal Yiou[1], Laurent Boissier[2, 3], and Arthur Perringaux[2]

[1]Laboratoire des Sciences du Climat et de l'Environnement, UMR8212 CEA-CNRS-UVSQ, Université Paris-Saclay & IPSL, 91191, Gif sur Yvette, FRANCE
[2]Generali France, 93210, Saint Denis, FRANCE
[3]Univ Paul Valéry Montpellier, LAGAM, F34000, Montpellier, FRANCE

Correspondence: Laura Hasbini (laura.hasbini@lsce.ipsl.fr)

Abstract. Winter windstorms cause extensive damage to infrastructure and represent the most significant natural hazard for Generali France in terms of insured losses. This study presents a method to systematically link physical storm events with observed insurance claims, enabling a better understanding of which storms, including weaker depressions, drive losses within Generali's portfolio. The proposed association may serve as a useful basis for the calibration of insurance and reinsurance processes such as risk assessment, loss modelling and prevention. Beyond analysing individual events, we assess the impact of storm clusters, defined as multiple storms affecting the same region within a 96-hour window, consistent with reinsurance contract definitions. Our findings reveal that 85% of windstorm-related losses since 1998 are attributable to clustered events. The most intense storms are frequently preceded or succeeded by smaller, yet damaging, depressions. This is illustrated by the case of Storms Anatol, Lothar and Martin in December 1999 and Storm Klaus in January 2009. Furthermore, we find that storms causing damage are more likely to occur as part of a cluster (50%) compared to the overall population of depressions affecting France (29%). These findings highlight the importance of accounting for storm clustering in risk modelling and reinsurance strategies.

1 Introduction

Extratropical cyclones (ETC) are a dominant meteorological phenomenon in the mid-latitudes, serving as key drivers of day-to-day weather and accounting for the majority of high-wind and precipitation events across Europe (Hawcroft et al., 2012). Windstorms are intense ETC associated with extreme wind events. In Europe, they rank among the costliest natural hazards with billions €of economic and insured losses per winter (ECMWF, 2024). Given their significant societal and economic impacts, windstorms have gathered considerable attention from climate sciences, meteorology, and insurance sectors. Physically, they are characterised by a storm track that follows the trajectory of the ETC. While various tracking algorithms effectively capture the general patterns of storm tracks, the choice of methodology significantly influences the number and characteristics of detected ETC (Neu et al., 2013). Each automated scheme is developed based on a specific conceptualisation of what best defines a cyclone, such as mean sea level pressure or relative vorticity at $850\mathrm{hPa}$. Additional criteria on the total length of the track, duration or intensity of the storms are also applied to constrain the set of tracks detected. Tracking algorithms typically

yield consistent results for intense cyclones and during phases of intense development within their life cycle. However, larger discrepancies arise during the genesis and lysis stages of ETC (Raible et al., 2008). Differences in the representation of the life cycle are particularly pronounced for weaker, slower-moving, and short-lived ETC (Flaounas et al., 2023). Additionally, absolute cyclone counts are highly sensitive to the chosen tracking methodology, which can lead to differences across studies (Neu et al., 2013).

To quantify the impacts of windstorms on society, several metrics have been developed. The most common one is the Storm Severity Index (SSI) introduced by Klawa and Ulbrich (2003). The SSI has been extensively applied in recent studies (Leckebusch et al., 2008; Lockwood et al., 2022; Priestley et al., 2023; Little et al., 2023; Cornér et al., 2024), providing a robust framework for assessing storm intensity and associated risks. However, it offers a restricted vision of the storms, as it focuses solely on the maximum wind speed relative to a given local wind percentile. In practice, the background dynamical environment, such as the presence of a strong jet stream (Hillier et al., 2025), and characteristics of the life-cycle, such as explosive cyclogenesis (Ludwig et al., 2015; Ginesta et al., 2023), duration and potential clustering, also play a crucial role in determining the spatial extent and severity of impacts. These additional aspects can provide a more comprehensive understanding of how storm characteristics translate into local-scale damage.

In Europe, the number of ETCs observed at a given location and over a specific period (ranging from an entire season to just a few days) can vary substantially, from seasons with no events to days or weeks experiencing multiple occurrences. The possible temporal concentration of cyclones at a given location is called cyclone serial clustering (Dacre and Pinto, 2020). However, no single, universally accepted definition of cyclone clustering exists. Variations in cyclone counts can, for example, be attributed to large-scale atmospheric dynamics or interaction between cyclones. Persistent conditions, such as an intense and zonal jet stream can lead to the serial clustering of cyclones (Pinto et al., 2014; Priestley et al., 2017b). Regions such as Western Europe, located at the exit and flanks of the North Atlantic storm track, are particularly susceptible to cyclone clustering (Dacre and Pinto, 2020). The concept of "cyclone families," first introduced by Bjerknes and Solberg (1922), further explains how the trailing conditions of a primary cyclone can facilitate secondary cyclogenesis through moist processes. Recent studies (e.g. Pinto et al., 2014; Priestley et al., 2020) have demonstrated that cyclones formed by secondary cyclogenesis are more numerous during clustered periods over Western Europe.

Serial clustering can be described by various metrics, with aggregation periods ranging from days to seasons. One commonly used is the dispersion statistic, defined as $\psi = \frac{\sigma^2}{\mu} - 1$, where μ and σ represent the mean and variance of cyclone counts over a given time interval (Mailier et al., 2006). This metric was introduced based on the observation that storm occurrences do not follow a Poisson distribution with constant intensity. While this relative frequency metric has the advantage of not being dependent on the local storm frequency, it does not provide comparable information suitable for impact assessment. In contrast, absolute frequency metrics, such as the count of cyclones over a fixed region and period, offer globally comparable data but are sensitive to the specific set of storm tracks used (Pinto et al., 2014, 2016). The choice of metrics depends on the research objectives. From an impact perspective, an absolute definition with a 96-hour window is particularly relevant for capturing the temporal clustering of extreme events, as it matches the event definitions commonly used in the reinsurance sector.

Clustering represents a major threat as it is especially pronounced for extreme cyclones in Western Europe (Vitolo et al., 2009). Notable examples include the winters of 1989/1990 (storms Daria, Herta, Nana, Judith, Ottilie, Hilie, Polly, Vivian, and Wiebke), 1999/2000 (storms Anatol, Lothar, and Martin) (Rivière et al., 2010), and 2013/2014 (storms Christian, Xavier, Dirk, Anne, and Christina) (Priestley et al., 2017a). These events caused significant material damage, which directly impacted the insurance sector. They also highlight the amplified risk associated with cyclone clustering and underscore the need for improved understanding and prediction of such phenomena.

The insurance industry relies heavily on the representation of hazard, as this underpins risk assessment, loss modelling and prevention. A correct characterisation of hazard-related damage is fundamental across several stages of the insurance and reinsurance process. Insurers seek to define events, which serve as the temporal periods over which claims are aggregated and reimbursed. These events are central to reinsurance contracts: claims falling outside an event definition are either not reimbursed or are covered through alternative mechanisms, often more costly. However, event definitions are typically based on claim dates and reported impacts rather than on the physical characteristics of the underlying hazard. As a result, they may lack physical coherence and are often adjusted to maximise the number of reimbursable claims, rather than to reflect a consistent hazard-based definition. A robust hazard characterisation would not only improve event separation but also enhance loss modelling and prevention. Insurers rely on historical loss data to estimate risk and to allocate capital for rare, high-impact events, such as those with 200-year return periods. By accurately linking damage to its physical drivers, it becomes possible to anticipate the potential losses associated with future events and to identify vulnerability factors that amplify impacts. This supports the design of targeted prevention and adaptation measures in the most exposed regions. Ultimately, improving the accuracy of hazard representation strengthens the physical consistency of event definitions and enhances the overall efficiency and reliability of both insurance and reinsurance processes.

Nonetheless, estimating storm impacts requires understanding the interplay between hazard, exposure, and vulnerability (Intergovernmental Panel On Climate Change, 2023). From this perspective, storms are often defined using surface wind intensity aggregated over multiple days (Moemken et al., 2024a; Severino et al., 2024). When combined with insurance loss data, this approach develops more robust damage models and vulnerability curves, which are essential tools for estimating expected losses (Prahl et al., 2015; Fonseca Cerda et al., 2024). However, this method presents key limitations: it does not capture the full cycle of the storms from the genesis to the lysis, nor the characteristics of its evolution, such as the deepening ratio, the translational speed or the total duration. Additionally, the temporal aggregation of wind data obscures the contributions of individual storms within clustered events. This makes it complicated to determine whether the observed impacts stem from a single, exceptionally damaging storm or from the cumulative effects of several storms occurring in close succession. As a result, current models often struggle to adapt to clustered events, where overlapping or sequential storms generate complex loss patterns that are not easily captured by traditional approaches.

Several datasets link storm damage to meteorological events, such as the Extreme Wind Storms (XWS) Catalogue (Roberts et al., 2014), PERILS (PERILS, 2025), the Copernicus Climate Change Service (Copernicus Climate Change Service, 2020) and Munich RE (Munich RE, 2025). While these datasets provide valuable insights, they often differ in the identified storms as well as in their loss estimates (Moemken et al., 2024b; Flynn et al., 2024). Designed primarily for reinsurance purposes,

they focus on the most impactful storms and provide smoothed loss estimates at regional or national scales. This limits their usefulness for detailed analyses linking storm intensity to localised damage. Working with primary insurance data, such as Generali France, allows for a more granular understanding of damage patterns, capturing a broader range of storm-related claims. Nonetheless, this raises the fundamental challenge of defining storm events based on damage databases (Kron et al., 2012). Stucki et al. (2014) demonstrate that temporally aggregated impacts can be extracted from such databases, though they are subject to biases, particularly those stemming from historical reporting practices and exposure variations. Despite these challenges, leveraging high-resolution claims data enables a precise damage assessment, distinguishing not only major storms but also individual members within storm clusters, offering a more refined perspective on impact patterns.

This study presents a method for linking high-resolution insurance claims to storm events, delivering practical value for both the insurance and meteorology sectors. From a meteorological standpoint, it can provide detailed insights into the atmospheric conditions contributing to damage and disentangle the impacts of successive storm events, thereby enhancing our understanding of storm clustering and its consequences. Accurately associating claims with specific storms is essential for impact research as it forms the basis for estimating storm-related costs, identifying return levels of costs, and calibrating vulnerability curves for different exposure scenarios. This paper addresses the following key questions :

- How can insurance claims data be linked to ETC?
- How can impact data be leveraged to distinguish the impacts of successive storms?
- What is the impact of short-duration storm clusters on insurance losses incurred by Generali France?

The paper is structured as follows. Section 2 characterises the dataset of Generali's claims, ETC tracks, and the method to identify clusters. The association method is described in Sect.3 with a sensitivity analysis and evaluated by comparison with other datasets. Section 4 examines the results of the association in the context of serial clustering, with two case studies including storms Lothar and Martin (Dec. 1999) and storm Klaus (Jan. 2009). Section 5 ends the paper with some perspectives and conclusions in Sect.6.

2 Data

2.1 Storm data

The study is performed with the ERA5 data (Hersbach et al., 2020). The dataset has a horizontal resolution of $0.25° \times 0.25°$, corresponding to $18\ \mathrm{km}$ at $50°\ \mathrm{N}$, and covers the period $1979-2024$ from October to March. Over such a dataset, storm tracks in the Northern Hemisphere were identified using the object-oriented algorithm TRACK algorithm (Hodges, 1999). First, the input data is smoothed over a $T42$ resolution (approximately $2.8°$) to filter out noise. ETC are then identified based on $6-$ hourly values of relative vorticity at $850\ \mathrm{hPa}$ connected with nearest neighbour search. No conditions are set on the total length of the trajectories, nor the minimal value of the maximal vorticity. We apply a spatial constraint to retain only storms impacting France. This is done by selecting the tracks with a maximal distance of $1300\ \mathrm{km}$ from the territory of metropolitan France. The

radius of $1300\ \mathrm{km}$ ensures that the largest depressions, which can have an impact, distant from the centre of maximal vorticity, are not discarded. The choice of the impact radius was motivated by previous studies (Hawcroft et al., 2018; Sinclair and Catto, 2023), who used a radius of 10° around the centre of minimal pressure; Copernicus C3S (2025) defined their footprints with a $1000\mathrm{km}$ radius. Although this radius may appear large for weaker depressions, we conducted several sensitivity tests using smaller radii and a variable radius conditioned on the minimum pressure observed throughout the ETC life cycle. Similar results were found with these additional tests and are developed in Sect. C. Additionally, only the well-developed depressions lasting more than 24 h are kept. This leads to a set of 4439 storms over the period ranging from March 1979 (included) until March 2024 (excluded).

For each identified track, we define the storm impact date (d_{storm}) as the date when the track is the closest to the longitude line of 7.5° W, where closest refers to the minimum Euclidean distance between the storm centre and this longitude. This point of closest approach, defined with respect to the 7.5° W longitude, is used as a reference to assign a unique identifier to each storm. The storm is named using its impact date and time, along with the latitude and longitude of its closest point. For example, Storm Lothar reached its closest point to the 7.5° W line on 26 December 1999 at $12:00$ UTC, located at 4.2° W and 51.5° N. It is therefore labeled as: *"1999-12-26 12h [-4.2;51.5]"*. This naming convention has been shown to uniquely identify storms, even in cases where multiple storms crossed the 7.5° W longitude on the same date, by incorporating both temporal and spatial characteristics of their trajectories. An example of two storms, their impact area and their naming with respect to the $7.5^\circ W$ longitude line, is illustrated in Fig.1. Storm footprints are defined using hourly $10\mathrm{m}$ wind gust with a circular spatial mask of $1300\mathrm{km}$ radius around the centre of maximal vorticity and a temporal window of $\pm 12\ \mathrm{hours}$ around each tracked point. Additionally, we defined the impact area of a given storm with a radius of $r\ \mathrm{km}$ moving with the centre of maximal vorticity.

The TRACK scheme has been shown to effectively represent ETC and is well-suited for impact analysis (Priestley et al., 2024, e.g.). However, we relaxed the conditions on cyclone duration and intensity compared to other studies (e.g. Priestley et al., 2024; Lockwood et al., 2022) which required a minimal cyclone duration of $48\mathrm{hours}$, a minimum track length of $1000\mathrm{km}$ and a minimal threshold of maximal vorticity of $10^{-5}\mathrm{s}^{-1}$. This was done to ensure the inclusion of more ETCs, particularly fast-moving and weaker storms, which can be responsible for significant damage locally. Priestley et al. (2020) also showed the importance of secondary cyclogenesis in serial clustering, which are often small-scale storms. Capturing storms of all scales is thus key for understanding damage during clustered events. The analysis is performed using a single tracking, which can present some limitations (Neu et al., 2013). Pre-restricting the set of storm tracks to only intense systems would bias the association, as claims could then only be linked to such events. Including depressions of all intensity, including smaller and weaker ETC, allows for a more exhaustive representation of the ETC that contribute to observed damage.

2.2 Serial clustering of storms

Definitions of storm clusters vary across the literature and typically depend on both temporal and spatial criteria. Previous studies have employed a range of approaches, including absolute frequency metrics (Pinto et al., 2014; Karwat et al., 2023; Hauser et al., 2023), relative frequency metrics (Mailier et al., 2006; Economou et al., 2015; Pinto et al., 2016), and different

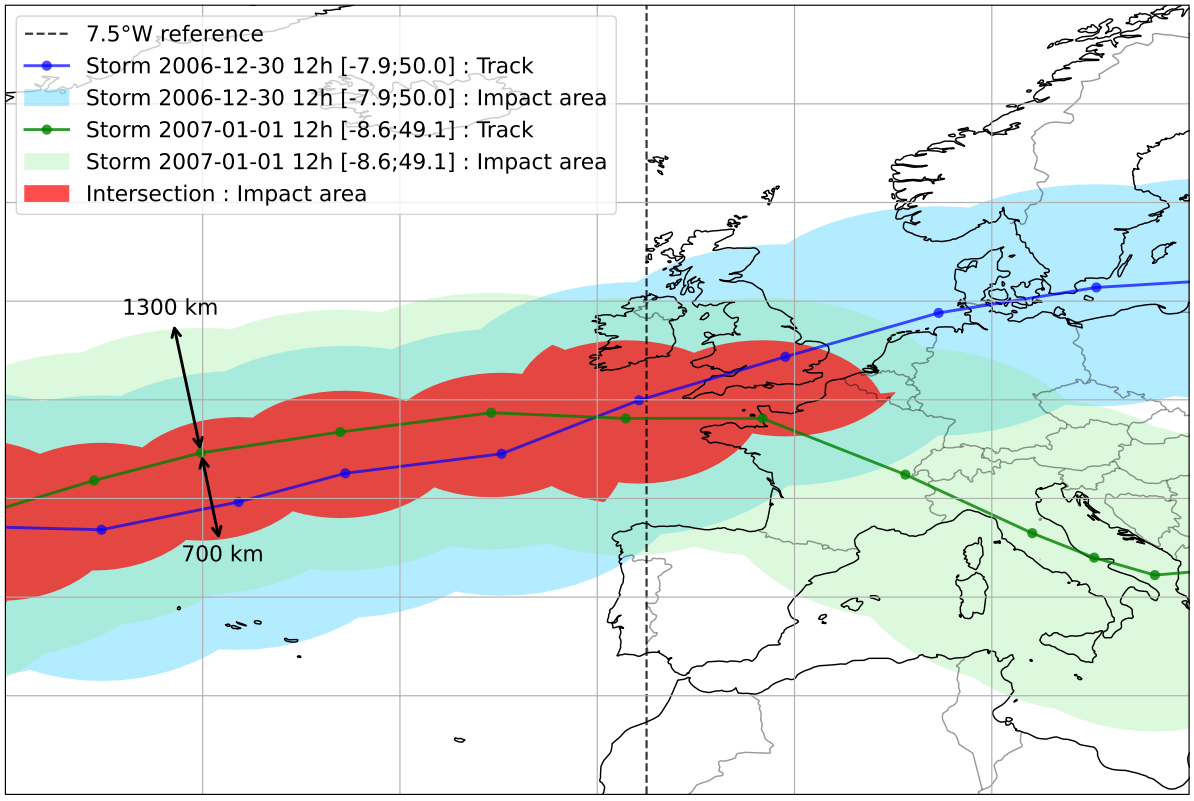

Figure 1. Example of clustering with two storms. The green and blue lines represent the storm tracks of storms 1 and 2, with 6-hourly time increments. The green and blue shadings represent, respectively, the impact area of storms 1 and 2, defined with a radius of 1300 km around the centre of the track. The red shading illustrates the intersection of "high-impact" areas, defined by a radius of 700 km around the storm tracks.

temporal windows (Dacre and Pinto, 2020). In this study, we adopt an absolute frequency-based approach, complemented by a spatial criterion. Specifically, two or more storms are considered part of the same cluster if their 700km-impact areas intersect, and their impact dates are separated by no more than 96h. The choice of a 700 km radius is based on the 6°angular distance around the centre of maximum vorticity, which has previously been used to define the region of strongest wind impacts (Zappa et al., 2013; Gramcianinov et al., 2020; Cornér et al., 2024). The radius is intentionally smaller than the one used to define the storm footprint in Sect.2.1, as the goal here is to capture regions exposed to the most intense wind gusts from multiple ETCs. Using a broader radius would risk merging most storms into clusters, and not having a significant set of individual storms. Figure 1 illustrates an example of a cluster with the tracks of the two storms, their own impact are (defined in Sect.2.1) and the intersection of these areas. The 96-h temporal window is consistent with storm definitions used in Generali's reinsurance contracts. To focus on events relevant to the French territory, we further require that the impact area intersection occurs over France. In cases where one identified cluster is entirely contained within another, the smaller (subset) cluster is discarded.

Under this definition, a single storm can be part of several clusters. Among the 4439 storms affecting France,1283 are part of at least one cluster. While one storm is found to participate in as many as 4 distinct clusters, the average is 1.18 clusters per storm. In total, 517 storm clusters are identified, with an average of 2.7 storms per cluster and a maximum of 13 storms in a single cluster.

2.3 Insurance data

Generali France's Property and Casualty (P&C) claims portfolio, spanning from 1998 to 2024, is used as the primary impact metric. From the most recent analysis of building insurance in France, the market share of Generali France can be estimated at 3% (Frédération France Assureurs, 2024a, b), which corresponds approximately to 1million of contracts. In France, residential property insurance is mandatory and coverage reaches nearly 99%. Consequently, Generali France's P&C claims portfolio provides a robust representation of storm-related residential property insurance impact. The analysis focuses on windstorm claims recorded during the extended winter season (September-April). Each claim is characterised by the geographical location of the damaged property, the date of declaration and the date of damage. In this study, we refer to the estimated date of damage as the claim date (d_{claim}). Damage intensity is quantified by the net insured loss, over which deductibles and coverage limits are truncated. As a result, some values may be zero or negative; these entries are excluded from the analysis. In addition, claims exceeding 150000€ in net insured loss at the date of damage, which correspond to "severe damage", are treated through a separate process and are also excluded. To ensure consistency across years, all monetary losses are detrended and converted to constant 2015 euros, written "$cst2015$", using inflation indices provided by the Institut National de la Statistique et des Etudes Economiques (INSEE, 2025). Claims can be categorised as closed, open or out of order. Closed claims have been paid based on the reported loss. Open claims are still under assessment, with losses subject to revision. Claims labelled as out of order, meaning not attributable to the relevant hazard, are excluded from the dataset. The full dataset was extracted on the 1st October 2024 and contains approximately 3% of opened claims, primarily corresponding to events in March and April 2024, at the end of the 2023/2024 winter season. After applying the filtering mentioned above, the cleaned dataset contains 210435 entries.

The geographical locations of insured properties are derived from textual addresses and converted into latitude and longitude using the Base Adresse Nationale, (Base Adresse Nationale, 2025), the national authoritative reference for French addresses. The geocoding tool from the Environmental Systems Research Institute (ESRI, 2025) is used to match addresses to this reference. Among the 210435 reported claims, 68% have a point level location match, meaning that the exact building is identified. For 23% of cases, only the street or hamlet name is identified. Lastly, $\approx 10\%$ have locations only determined at the postcode level.

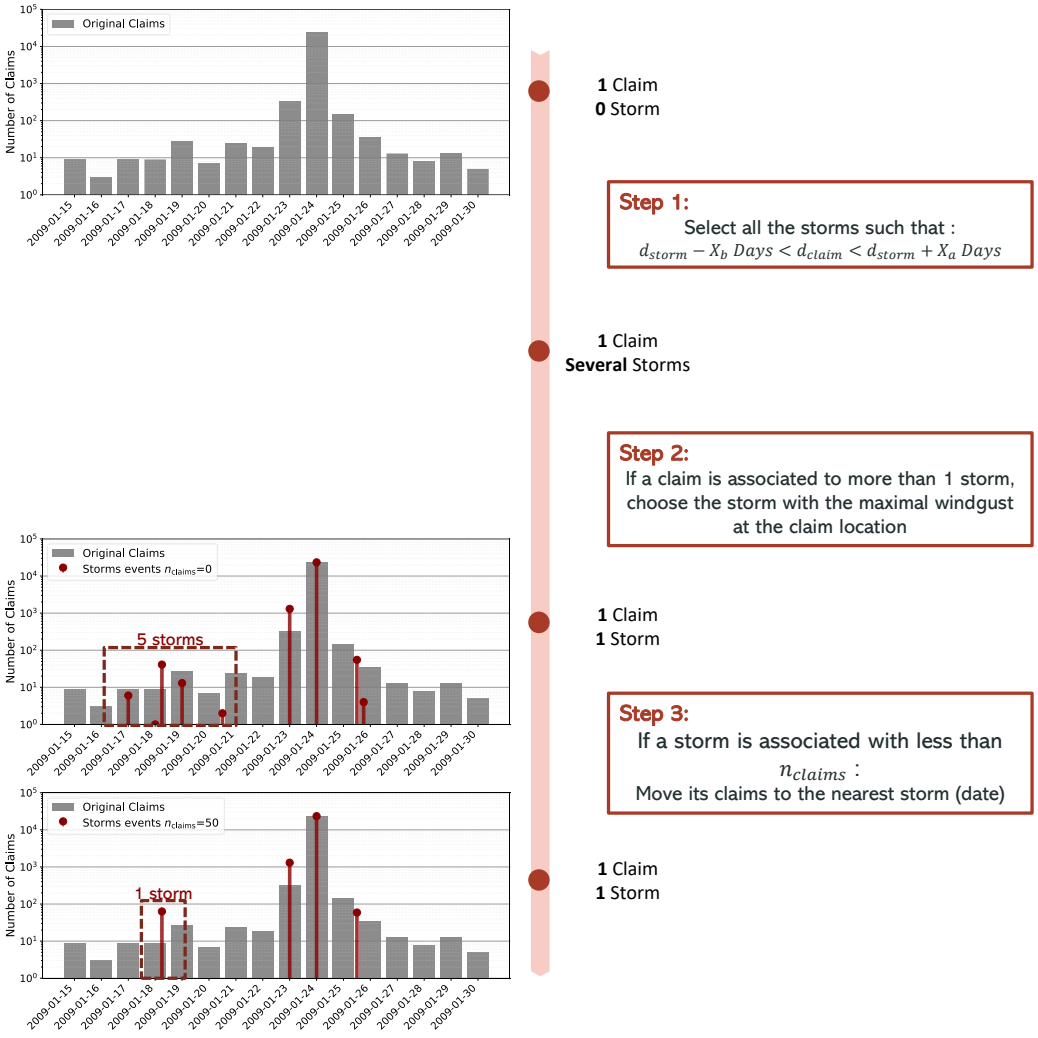

Figure 2. Schematic of the association process between claims and storm events for the case study of Sect.4.2. Plots on the left show the evolution of claims and their associated storms at every step of the association. Grey bars represent the number of claims per day, dark red lines show the storm events and their associated number of claims. The last two histograms make a focus of the beginning of the time period over which 5 storms could be responsible for claims but one is kept, and linked to less than 100 claims at the final step of the association. Panels on the right

3 Methods

3.1 Association of claims to storm events

Claim dates filled in the damage dataset are inherently biased as they are reported by policyholders based on their perception and interpretation of the hazard. Known as historical perception, the raw loss dataset tends to over-represent intense windstorms and under-represent the ones of smaller intensity (Stucki et al., 2014). This is exacerbated by the identification of storm dates, which cannot be used as a reliable identifier without pre-processing. The usual strategy is to aggregate the damage over several days, as done by Stucki et al. (2014), but this erases the contribution of smaller-scale storms. To address this data quality issue while still capturing the impact of all ETC events, we propose an association strategy that maps the claims and the storms accurately.

The first step consists of linking each claim to all storms with an impact date close to the claim date. This closeness is determined by a temporal window defined by several days before (X_b) and after (X_a) the storm date (d_{storm}). Concretely, storms are selected so that their impact date d_{storm} verifies $d_{\mathrm{storm}} - X_b \leq d_{\mathrm{claim}} \leq d_{\mathrm{storm}} + X_a$ (in days). Here, d_{claim} is the date of occurrence of the claim. This initial selection may link a claim to one or multiple storms.

Since the ultimate goal is to associate each claim with a single storm, the storm most likely resulting in the damage will be chosen following a method based on wind gust value. Each claim is linked to the storm with the highest wind gust value at the claim location. The second histogram of Fig.2 illustrates the resulting storm-claim associations, showing for each identified storm the number of claims attributed to it. While a good alignment is observed for the major events on the 23rd and 24th of January 2009, between the 17th and the 21st, five potential storm candidates are identified, some of which are associated with fewer than 10 claims. Given that storm systems are typically large-scale events and that Generali's exposure is broadly representative of the French market, it is unlikely that a storm would result in fewer than 50 claims. As this threshold is arbitrary, we introduce it with the variable n_{claims} that will be optimised to better match the observed impact. If a storm is associated with fewer claims than this minimum, its damage is reassigned to the closest storm in terms of date. This process is repeated iteratively, increasing the number of claims by 10 each time, until reliable results are achieved. The last histogram of Fig.2 shows the storm events identified after the last step of this association strategy.

The proposed association depends on three tuning parameters X_b, X_a and n_{claims}, respectively corresponding to the number of days before the storm date, the number of days after the storm date and the minimal number of claims associated with a storm. These parameters help fine-tune the association between claims and storms. The performances of the association are evaluated with three metrics, comparing the identified storms to the claim's local maxima. The local maxima are identified by peaks over the time series of claim count gathering at least 10 claims. The tuning of the association assumes that the loss data correctly captures the major physical events, although they can present some temporal shift. The local maxima identified using the distribution of the number of claims as a function of time represent the target of the association. The constructed metrics evaluate whether the number of storms corresponds to the number of peak claims and whether the claim peak dates are not too far from the actual storm impact date. The precision metric (M_{days}) is computed as the maximal difference between a storm date and its closest local maximum, in terms of date. The smaller this difference, the better the association. The

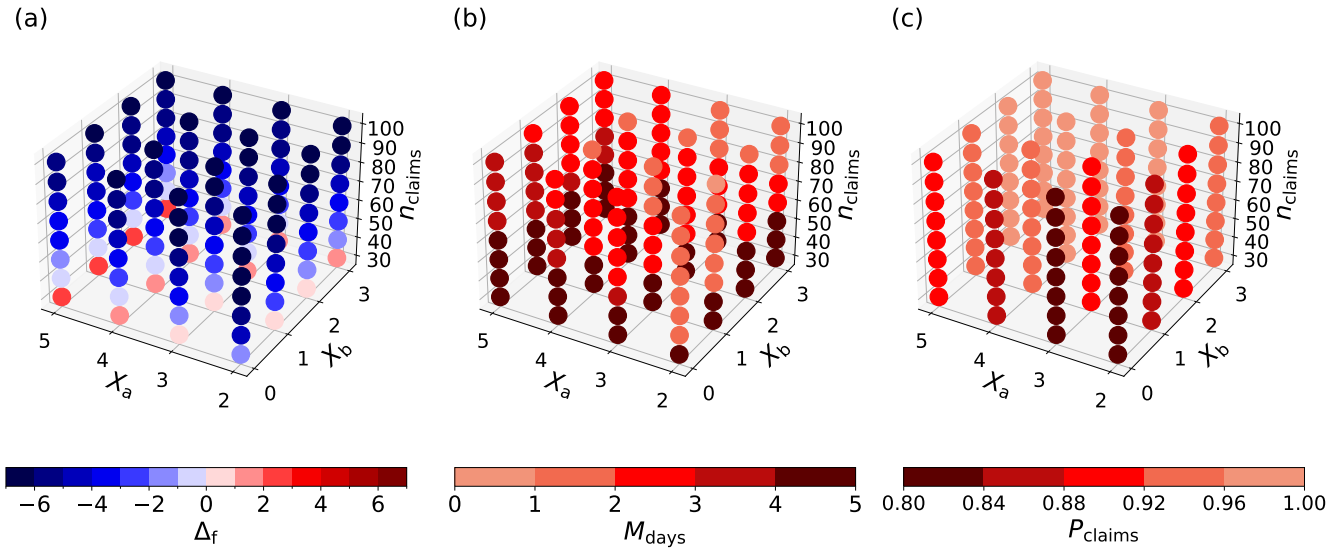

Figure 3. Frequency (Δ_f) in number of events (a), precision (M_{days}) in number of days (b) and completeness (P_{claims}) in percent (c) as a function of X_a (horizontal x), X_b (horizontal y) and n_{claims} (vertical z). The optimal set of parameters(X_a, X_b, n_{claims}) is obtained when the difference is null.

frequency metric (Δ_f) is defined as the difference between the number of storms compared to the number of local maxima. Lastly, a completeness metric (P_{claims}) corresponding to the percentage of claims associated with storm events is defined. These metrics collectively provide a robust evaluation of how well the association strategy maps claims to storms, ensuring both accuracy and completeness in the analysis. No spatial performances are evaluated at this stage. It is assumed that the conditioning on the storm with the highest wind gust should already capture the spatial distribution.

In mathematical terms, let $\{S_1, \ldots, S_n\}$ be the dates of the storms identified and $\{L_1, \ldots, L_m\}$ the dates local maxima. Then the frequency difference is defined as $\Delta_f = n - m$. The precision metric can be written as $M_{\text{days}} = \max_{j \in [1,n]} \min_{i \in [1,m]} |S_j - L_i|$. The difference between the dates $|S_j - L_i|$ is expressed in days, as the local maxima computed over the claim dates are at the day level.

3.2 Sensitivity of the association to parameters

This subsection inspects the evolution of the performance metrics as a function of the tuning parameters. The performance metrics are computed independently for each winter and for X_b in $\{0,1,2,3\}$, X_a in $\{2,3,4,5\}$ and n_{claims} between 30 and 100 with 10 claims steps. The metrics are then averaged over all the winters. Figure 3 shows the evolution of the frequency, precision and completeness metrics as a function of the tuning parameters. Lighter colours indicate better results.

The impact of the association windows can first be analysed. If X_a is too large, the precision decreases with a bigger minimal difference between the storm date and the closest local maxima date (Fig. 3b). Conversely, increasing X_a enables the

capture of more claims, thus being more representative of the global dataset (Fig. 3c). In terms of performance, this improves the completeness metric. Nonetheless, we see that the variation in the completeness varies less than the precision metric. The behaviour of X_b is similar to that of X_a. A greater value would allow for more completeness, but would also decrease the precision of the association. The n_{claims} parameters do not alter the completeness performances. This parameter defines the threshold under which claims should be shifted; it thus does not influence the number of claims linked to some storms. Regarding precision (Fig.3b), shifting claims reduces the maximal difference between storm dates and the nearest peaks. This underlines that the shifted claims seem to be those farthest from the peak dates

The behaviour of the frequency metric is more complex as it depends on the interaction of the 3 parameters (Fig. 3a). For a given window, increasing the minimal number of claims (n_{claims}) reduces the number of storms and consequently decreases the Δ_f. This reduction is needed when a positive frequency is observed. When more storms are detected than the number of local maxima. However, decreasing it too much leads to a negative one. This corresponds to over-concentration around the major storm events, with more local maxima than the number of storms. The situation when too many storms are captured (positive Δ_f) is mostly observed when n_{claims} is small.

A trade-off should be found between the size of the association windows (X_a and X_b) and the strength of the concentration over the major events (n_{claims}). The optimal association should not only be complete but also associate the claims with their correct storms. Fig. 3c shows that the smallest percentage of claims that can be linked to storm events is 80%. As this is already satisfactory, the quality of the linkage will only be measured using the difference in frequency and the maximal temporal difference between storm events and local maxima.

The optimal tuning parameters X_b, X_a and n_{claims} are found by minimizing the cost function defined as :

$$f_{cost}(w_{freq}) = \sqrt{w_{freq} \times \Delta_f^2 + (1 - w_{freq}) \times M_{\text{days}}^2}. \tag{1}$$

The frequency and precision metrics are centred between 0 and 1, w_{freq} is a weight attributed to the frequency metric, which can vary between 0 and 1. This weight is used to quantify the sensitivity of the optimal parameters found. Optimisation is performed over f_{cost} using global minimization search for $(X_a, X_b, N_{\text{min\_claims}}) \in \{0,3\} \times \{2,5\} \times \{30,100\}$. The robustness of the results to w_{freq} is developed in Sect. C.

Minimising the loss function leads to $X_b = 3$, $X_a = 3$ and $N_{\text{min\_claims}} = 50$. Such parameters will be kept for the rest of the study. The obtained window of 7 days is comparable to the one of 5 days used by Fonseca Cerda et al. (2024). We expect that such large windows will better account for the potential postponed impact of a windstorm but also for the error made by the insured person when declaring the damage date. Additionally, the linking strategy based on the maximal wind-gust value should ensure the association with the correct storm driver.

3.3 Representativity of the catalogue

Assessing the representativeness of the resulting catalogues remains a methodological challenge due to the variety of available approaches. In a comparison between academic and insurance-based catalogues, Moemken et al. (2024b) highlight significant discrepancies in storm frequencies, major event identification, and estimated losses. These differences stem from the primary

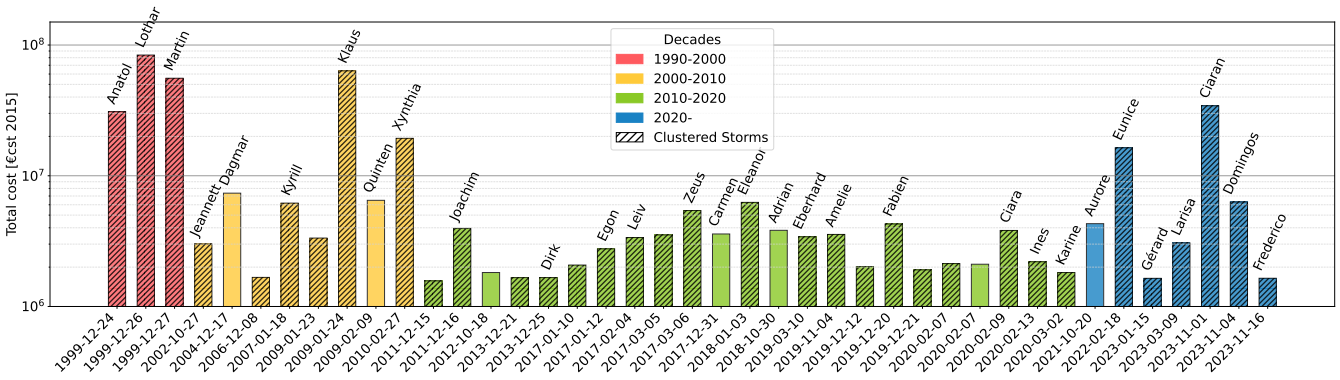

Figure 4. Losses in constant € 2015 of the 40 costliest storms for Generali France over the period $1998 - 2024$. Storm dates are indicated in the x-axis and Storm names over the bar plot of each event. Colours indicate the decade during which the storm event occurred. Dashed bars indicate storms being part of a cluster.

objectives of each catalogue but may have important implications for risk assessment. The proposed approach, especially tailored to Generali's exposure, should result in the most precise and accurate catalogue.

A key consideration is the dataset ability to accurately capture the most severe historical events. Applying the association method described above, 335 storms are associated with an impact for Generali over the $1997 - 2024$ period. We call these events impacting storms. Among these, the 40 costliest events are presented in Fig. 4. Notably, storms Anatol, Lothar, Martin, Klaus, Xynthia, Eunice, and Ciaran were the most costly for Generali, with losses exceeding 10M€ per event. Importantly, our method successfully captures high-impact storms documented in global datasets (PERILS, 2025; Flynn et al., 2024; Copernicus Climate Change Service, 2020), as evidenced in Fig. 4. Further comparison with Météo France's catalogue, produced using the SSI, reveals a strong agreement over the period 1998–2024 (Meteo France, 2023). Only the storms of 16-17 December 2019 (storm Andrea and Calvann) rank among the most intense in Météo France's analysis, but do not appear in the top 40 costliest events from Generali. This discrepancy warrants further investigation, with one plausible explanation being the influence of Generali's portfolio.

The resulting catalogue exhibits a great yearly variability in both the number of impacting storms and in losses amount. Fig. 5 underlines that the costliest winter seasons do not always correspond to the year with the most numerous storms or clusters. This is especially the case for the winter $1999/2000$ with only 7 storms associated with damage, but corresponding to the costliest winter. The winter $2013/2014$ is also notable with 21 storms identified with damage, but a total loss for the season close to the average. This high number of storms associated with moderate losses can come from the diversity of our storm tracks. As small and fast-moving depressions were kept in the set of storm tracks, it is more likely to encounter small storms associated with little losses. The variation of losses can be explained by both the intensity of the storms and the vulnerability of the areas exposed. This underscores the complex interplay between meteorological variability and socioeconomic vulnerability.

The pronounced interannual variability in the number of ETCs is consistent with the intrinsic characteristics of these systems, as highlighted by Feser et al. (2015). Furthermore, Moemken et al. (2024b) emphasises that this variability can become even

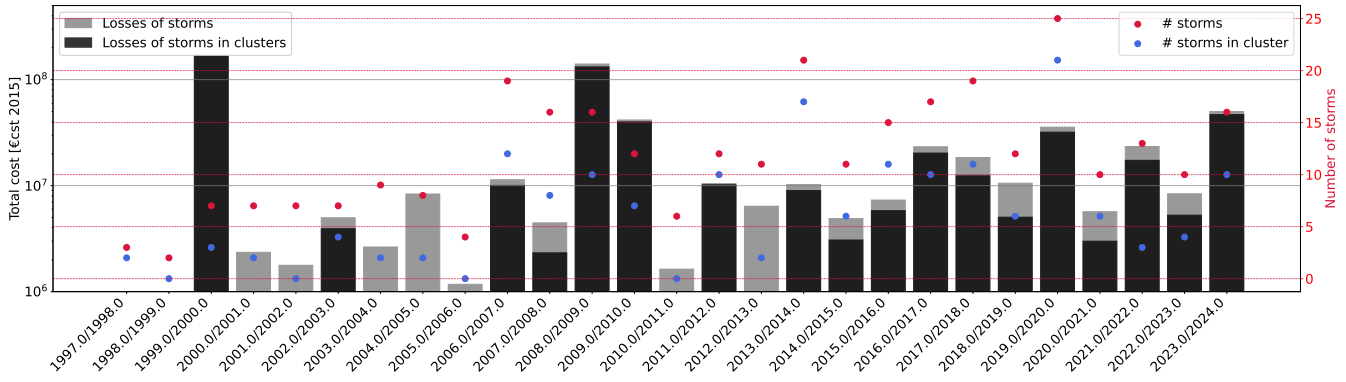

Figure 5. Yearly insured losses and storm occurrences. Light gray bars represent the total losses in constant € 2015 per winter season; darker bars indicate the amount linked to clusters of storms. The points represent the number of storms (red) and the number of storms being part of clusters (blue) per winter season. Winter y to $y+1$ starts from September of year y and ends in March of year $y+1$

more pronounced when considering storm-related losses, due to their strong dependence on varying exposure levels from year to year. The patterns of interannual variability in both storm counts and associated losses, as illustrated in Fig. 5, are therefore in line with previous findings in the literature.

The quality of the dataset can be evaluated using insurance-based metrics. The catalogue should reproduce the global damage statistics of storms. Fig. 6 illustrates the distribution of the total cost per storm, the mean cost per claim and the number of claims per storm. Such metrics are computed after aggregating policy-based costs at the storm level. An important difference can be found between the mean and median for both the total cost (Fig. 6a) and the number of claims per storm (Fig. 6c). Such differences are related to the heterogeneity of storm costs. The most intense storms, associated with long return periods, correspond to outliers of the main distribution. Frédération France Assureur (2025) estimated a mean cost of varying between 1530 and 2335 in constant € of 2023 for residential properties. This corresponds to a range of $[1285, 1962]$ in constant € of 2015. These values are lower than our mean estimate of 2700€ in Fig. 6. Mission Risques Naturels (2021) performed an in-depth study but only over the winter $2018/2019$. Their results underline that the average cost greatly depends on the type of infrastructure impacted. The gap with the observed mean damage in Fig. 6 can also be explained by the exposure of Generali as well as the historical depth. Generali is mostly implanted in the cities (Paris, Lyon, Lille, Bordeaux), the South-East of France and in the North.

4 Results: Impact of storm clustering

4.1 Case Study of December 1999: Storms Anatol, Lothar and Martin

The winter of 1999 represented a significant challenge for the insurance sector in Europe, particularly in France, due to the successive storms Anatol, Lothar and Martin on the $24th$, $26th$ and $27th$ December 1999. Storm Anatol had a northern trajec-

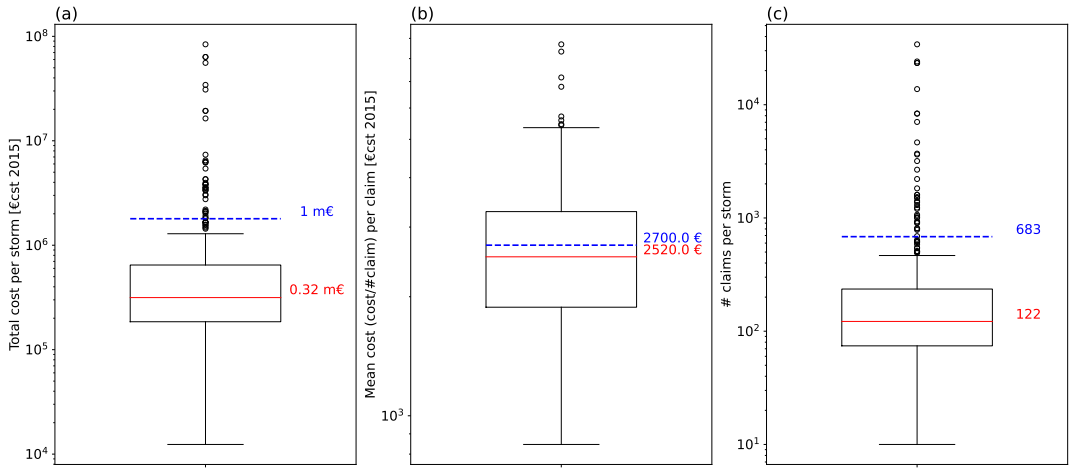

Figure 6. Distribution of the total cost per storm in constant € 2015 (a), the cost per claim in constant € 2015 (b) and the number of claims per storm (c). Red lines indicate the median, and blue dashed ones the mean.

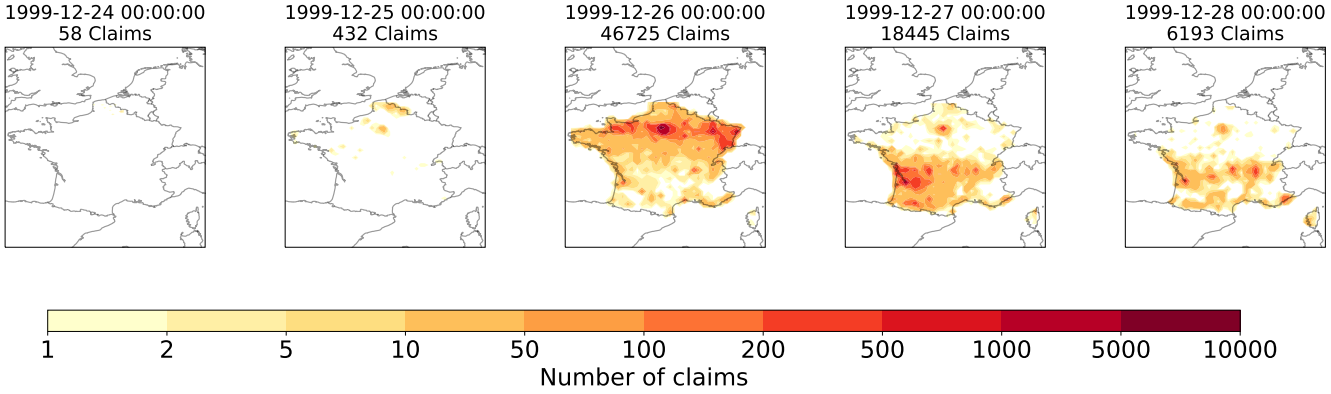

Figure 7. Map of the number of claims per day from 24/12/1999 until the 28/12/1999

tory, causing severe damage across Scandinavia (Kettle, 2021). Lothar, meanwhile, brought widespread destruction to France, Switzerland (Bründl and Rickli, 2002), Germany (Schmoeckel and Kottmeier, 2008; Schindler et al., 2009), and Belgium. Storm Martin followed a path similar to that of Lothar, leading to an exacerbated impact in the regions mentioned previously.

The presence of a strong upper-level zonal jet facilitated the formation of these storms (Wernli et al., 2002; Rivière et al., 2010). With only 24 hours separating them, their impacts are difficult to distinguish in aggregated data. At the time, the reinsurance 72 hour clause was loosened for recovery purposes and allowed for separating some losses (Risk Management Solutions, Inc, 2000). Nonetheless, this distinction was made solely for economic constraints and was not based on the actual damage caused by each storm. As a result, most studies treat Lothar and Martin as single events when evaluating their collective impacts (Michèle Lai, 2019; Welker et al., 2021).

Studies have underlined difficulties in disentangling the individual impacts of these storms. Fig. 7 illustrates the spatial distribution of claims per day. It highlights the impossibility of differentiating between storms Anatol, Lothar and Martin using claim date only. Fig.7 illustrates the spatial distribution of claims around the dates of both storm events. We can underline that claims were declared for each of the days and over the whole of France during the subset period. For cities such as Paris, claims were identified each day. Without more information about the intensity and location of the storms, it is thus impossible to differentiate between the successive events.

Storm Anatol, Lothar and Martin respectively had an impact on the $24th$, $26th$ and $27th$ December 1999. However, no claims were declared on the $24th$ and the impact of Lothar and Martin is likely mixed with the claims declared between the $26th$ and the $28th$. Restricting the analysis to claims reported strictly on the date of each storm would risk mis-attributing impacts. Such mis-attribution can compromise the accuracy of vulnerability curves by linking damages to incorrect meteorological conditions. Furthermore, attributing claims to the wrong event and date may affect the proper aggregation of losses under the $96\mathrm{h}$ reinsurance clause.

We applied our association method using the maximum gust wind speed of the three storms and the insurance claims for the period between Dec. 20 and Dec 30 1999 ($X_a = X_b = 3$ days). 1514 claims (out of 73605) cannot be attributed to any of the three storms. Fig.8 shows the footprints of storms Anatol, Lothar and Martin along with their associated claims. The distinction between their estimated impacts is particularly evident over central France and corresponds well to the shift of the highest wind gust. Our association procedure leads to a better focus on the impact regions of successive events, allowing us to distinguish their effects even when storms share a common impact area. Hence, the claim patterns Fig.7 can be refined to those in Fig.8.

We underline that the three storms have resulted in some damage in Paris. Although Storm Lothar had the highest windgust in the Paris area, the claim date played a key role in the distinction. This means that the claims observed in Paris and attributed to storm Anatol must have had a claim date earlier than December 23rd 1999 ($X_b = 3$ days before the impact date of storm Lothar). Similarly, the claims observed in Paris and attributed to storm Martin must have been declared later than $X_a = 3$ days after storm Lothar, so later than December 29 1999.

We highlight that damage is separated solely by the most intense wind gust. Our approach does not account for the persistence of strong wind gusts or the possibility that damage may result from the last storm, even if it did not produce the highest wind gust. This represents the primary limitation of the method. An alternative approach could involve using a different association method, such as linking events based on the closest track in terms of distance. However, for clustered storms affecting the same region, this may not be ideal. As illustrated in Fig. 8, weaker wind gusts can be observed near the centre of maximum vorticity. This suggests that some damage could be incorrectly attributed to areas with relatively low local wind gusts.

Although usual reinsurance gathers storm events with a 72 or $96\mathrm{h}$ time difference, in case of major events such as Lothar and Martin, separation could be needed. The association also succeeds in capturing postponed damage that could be declared a few days after the storm event.

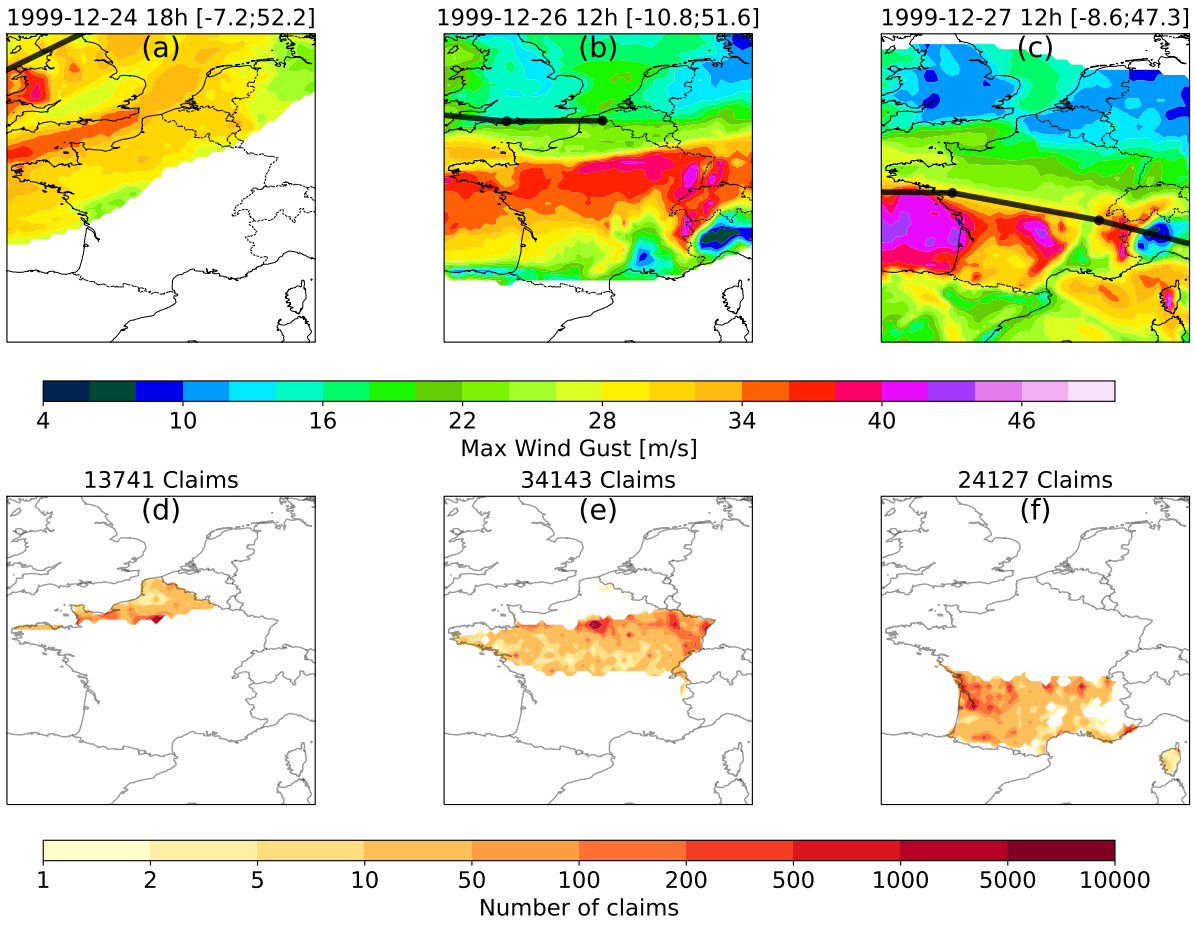

Figure 8. Association of claims to storms. Each column contains the maximum wind gust speed and the number of claims associated with a storm in Dec. 1999. Panels (a) and (d) show maps obtained for storm Anatol (*"1999-12-24 18h [-7.1;52.1]"*, (b) and (e) for storm Lothar (*"1999-12-26 12h [-4.2;51.6]"*) and (c) and (f) for storm Martin (*"1999-12-27 12h [-5.2;49.4]"*). Panels (a), (b) and (c) show wind-gust footprints and the storm trajectories (thick black lines), panels (d), (e) and (f) show the spatial distribution of the number of claims associated with each storm, while titles indicate the total number of claims for the whole event.

4.2 Case Study: Storm Klaus

The storm–claim association also underlines the relative contribution of smaller storms, which are usually discarded. As discussed in Sect.2.1, it is crucial to account for all storms, as fast-moving systems or smaller depressions can generate strong surface winds. If these storms are not captured, all the damage may be attributed to the strongest storm, which might not be the one responsible for the winds at a given location. The example of Storm Klaus serves to illustrate the importance of including small depressions and accurately distinguishing their impacts.

Storm Klaus affected Southern France and Northern Iberia between January 23 and 24, 2009. It was characterised by an explosive deepening of 37 hPa within 24 h, which is relatively uncommon for this latitude (Liberato et al., 2011). This rapid intensification was driven by an extended and intense polar jet at upper levels. At the surface, strong wind gusts caused significant damage to infrastructure and forests (AIR, 2009).

This storm is often treated as a standalone event by many insurers. Claims filed within a 72 or 96 hour window around January 24, 2009, are typically attributed solely to Klaus. However, our association results reveal that Storm Klaus was part of a broader storm cluster. The tracking algorithm identified a preceding depression, which will be named Storm A, crossing Northern France on January 23, 2009, which produced significant wind gusts exceeding 20 m/s in central and northern France. Additionally, a secondary low-pressure system developed on January 25, 2009, that we named Storm B, was potentially responsible for claims in the South-West of France. As illustrated in Fig.9 and 10, wind gusts generated by the January 23 and January 25 ETCs exceeded those generated by Klaus in several regions. This suggests that damages in northern and central France may not be attributable to Klaus alone. These findings demonstrate the added value of our storm-claim association method and highlight the importance of including smaller depressions in storm databases.

This example demonstrates the importance of the accurate storm–claim association, especially in cases of clustering. Attributing all impacts to Storm Klaus neglects the influence of smaller depressions. The relative contribution of these small systems within a 96-hour cumulative sum is essential for understanding the role of serial storm clustering. This study highlights potential pitfalls in the interpretation of clustered events, as aggregated losses, claims, or impacts over a period as large as 72h or 96h often encompass damage from multiple storm events. It remains unclear whether Klaus alone would have caused similar levels of damage had it not been preceded by another system, a consideration critical for understanding compound and cascading impacts.

4.3 Global statistics of storm clustering impacts

The clustering method described in Sect. 2.2 can be applied to the set of impacting storms. This identifies events such as storms Lothar and Martin in 1999, when at least two storms were responsible for damage. We call these events high-impact clusters. Over the ensemble of 335 storms associated with impact for Generali, we found that 167 of them are divided into 75 high-impact clusters. This corresponds to a ratio of $\approx 50\%$, greater than the one of 29%, found when applying clustering over all the storm tracks. It means that the most impactful storms are more frequently part of clusters. Although such storms are not the most numerous, they result in most of the damage. It can already be seen in Fig. 4 that from the 40 most costly storms for

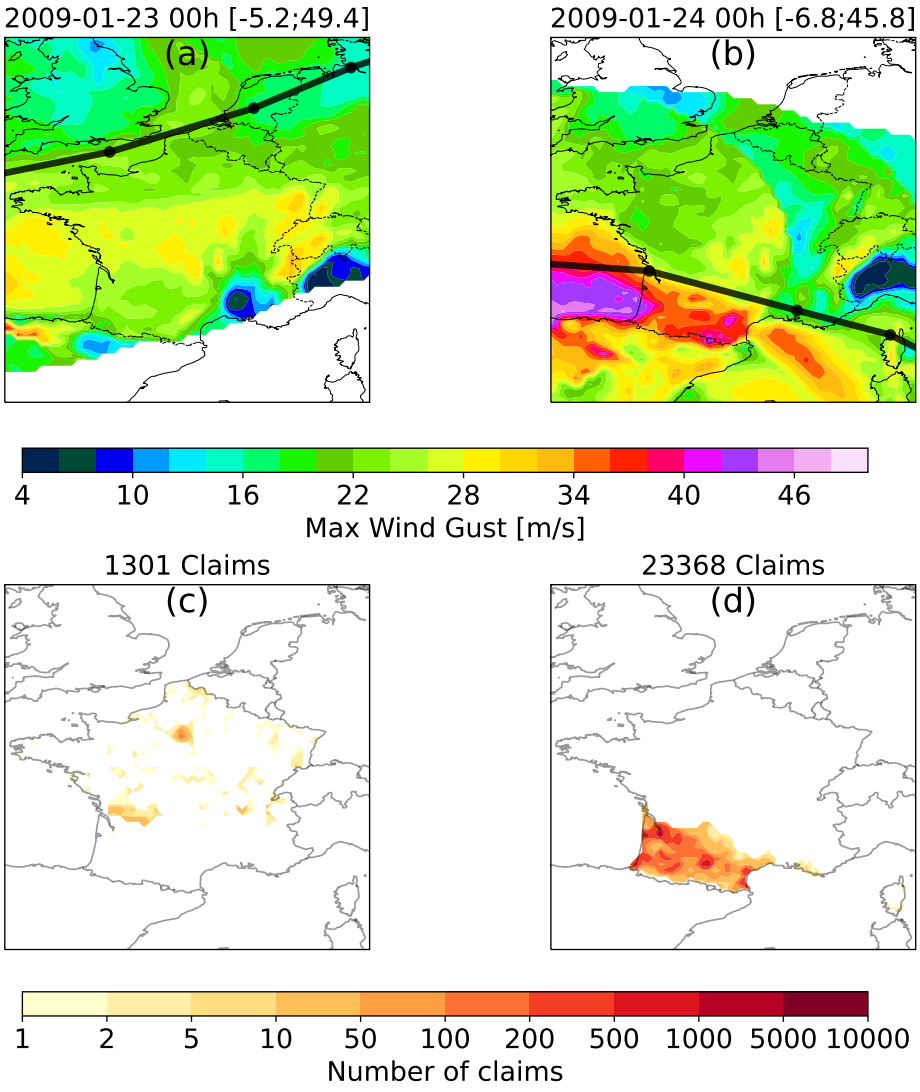

Figure 9. Same as Fig.8 with storm A(*"2009-01-23 00h [-5.2;49.4]"*) in panels (a) and (c) and storm Klaus (*"2009-01-24 00h [-6.8;45.8]"*) in panels (b) and (d).

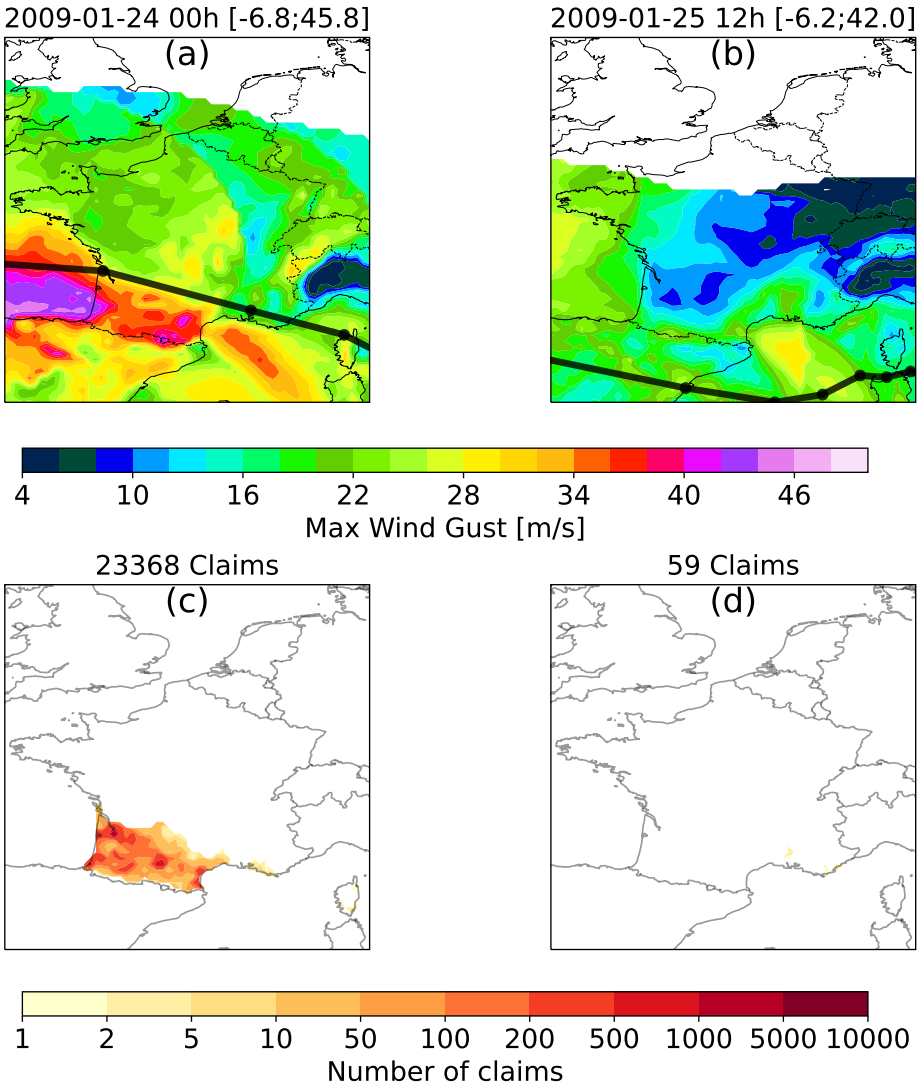

Figure 10. Same as Fig.8 with storm Klaus (*"2009-01-24 00h [-6.8;45.8]"*) in panels (a) and (c) and storm B *"2009-01-25 12h [-6.2;42.0]"* in panels (b) and (d).

Generali, 82% are part of a cluster. Extending this to the full dataset, we found that clusters of storms are responsible for 85% of the total windstorm loss and declared claims, which is greater than their physical occurrence frequency. Storms in clusters thus seem to be more frequently impacting, but also more costly.

Section 3.3 underlined that storm count and losses exhibit significant yearly variability. This is also the case for storm clustering. The period from 2000 to 2005 experiences a few impactful storms for Generali, resulting in moderate losses. Conversely, the last 10 years from 2013 to 2023 were associated with important storm losses and a particular importance of clustering. Interestingly, the number of storms in clusters observed in each season is not the main driver of the loss. We note the winter $2021/2022$ with only 3 storms in clusters, but accounting for most of the loss. As already pointed out in Sect.3.3, this is a signal that the damage associated with the smaller depression is also captured. During the winters of 1999, 2008, 2009, 2019 and 2023, which are the costliest in record for Generali France, almost all the losses are associated with storms in clusters. Over each season, major storms can be identified, such as storms Anatol, Lothar and Martin in $1999/2000$, storm Klaus in $2008/2009$, storm Xynthia in $2009/2010$, storms Amelie, Fabien, Ciara, Ines and Karine in $2019/2020$ or storm Ciarán, Domingos and Frederico in $2023/2024$.

Figs. 4 and 5 together emphasise the importance of an event-based analysis. What drives the loss is not only the clustering phenomenon but also the storm itself. To understand the importance of the clustering phenomenon in the repartition of the loss, we investigate how the loss is distributed within a cluster. For each storm member of a cluster, we compute its share of the loss as the total cost of one of the storm events divided by the total cost of the cluster. We can compare this value to the loss and occurrence rank. A loss rank of 1 corresponds to the costliest member of the cluster; similarly, an occurrence rank of 1 corresponds to the earliest storm of the cluster.

From the 75 cluster events identified, Fig.11 shows the share of the loss as a function of these ranks. Fig.11a highlights a great spread of the loss within the several clusters, the costliest storm can be responsible for between 41 and 99% of the total cluster losses. On average, we found that the costliest storm of the cluster represents 70% of the loss of the total event, indicating that a single storm generally dominates the overall cost. Nonetheless, the remaining share of losses still reflects a significant contribution from additional storms within the same cluster, underlining the need for insurance to group storms around clusters. This suggests that the total observed damage often comes from the temporal clustering of such events.

Fig. 11b shows that the order of arrival of the storms is not a driver of the loss. On average the first storm of the sequence is worth 40% of the total cluster loss, but this amount varies greatly from almost no impact to the total impact of the cluster. The same can be said for the $2nd$ storm. Lower values are found for the $3rd$ and $4th$ storms. However, we note that fewer cluster events are found with more than 2 storms. Additionally, an equally split loss corresponds to 30% and 25% of the total cluster loss when the cluster counts respectively 3 and 4 members.

We can note that the median and the mean are almost identical for all the box plots. This suggests the percentage of cluster loss follows a Gaussian distribution for all the given losses and occurrence ranks. The most extreme storms consequently do not exhibit specific statistics concerning these variables, as opposed to what was observed with event-based analysis in Fig.6.

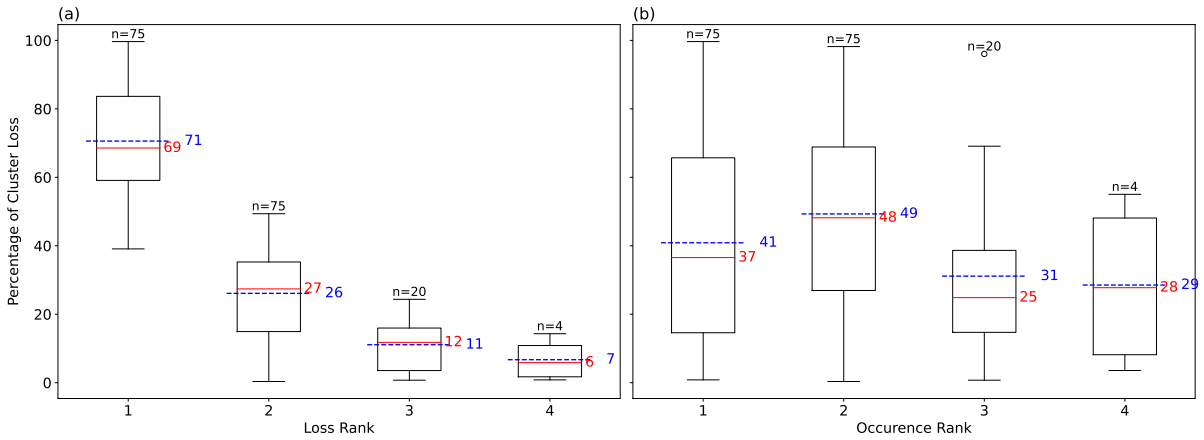

Figure 11. Distribution of the loss within the members of the cluster as a function of the loss (a) and occurrence rank (b). Thick red lines indicate the median, and blue dashed ones the mean. The numbers above each box correspond to the number of clusters used for each box plot.

Finally, the near-equality of the medians and means in the box plots suggests the distribution of cluster losses by loss and occurrence rank is approximately normal. Unlike the event-based results in Fig.6, the most extreme storms do not show distinct statistical behavior in this cluster-based view.

A similar analysis can be applied to frequency (Fig. D1), represented by the number of claims per event. The results are comparable: on average, the most impactful storm accounts for 68% of the total claims, with substantial variability in the share of claims across different claim ranks. Fig.D1 also indicates that the order in which storms occur within a cluster does not appear to influence how claims are distributed among the storms.

5 Discussions and perspectives

Extracting quantitative impact information from insurance claims presents significant challenges. While such data provide a direct measure of socioeconomic impact, it is often influenced by variations in insurance exposure, both spatially and temporally. The raw nature of claim data introduces potential quality issues. Reported damages depend on the awareness of policyholders and claims managers, who may be influenced by external factors such as media coverage of the event. This leads to an under-representation of smaller or moderate windstorms, a phenomenon referred to as "historical perception bias" (Stucki et al., 2014). Additionally, the occurrence and severity of damage cannot be fully explained by physical storm variables alone, because socio-economic factors and inherent randomness also play roles (Birkmann et al., 2013). Careful post-processing was therefore essential to extract meaningful signals from claim databases.

This study introduces a robust methodology to associate high-resolution claims data with ETCs, enabling a more accurate attribution of damages. The method is based on three tunable parameters: a temporal window around storm occurrence (X_b

days before and X_a after) and a minimum claim threshold (n_{claims}) to identify impactful events. Applied to windstorm claims from Generali France, the optimal window of three days before and after storm events and a gathering around storms with at least 50 claims effectively captures the storm-related damage signal. While the method was tested on the claim data from a single insurer in France, its design is adaptable to other perils, portfolios, and regions. The simplicity of the tuning parameters makes the method highly transposable to other hazards (e.g. flood, convective storms) as well as other types of damage (e.g. hail, water infiltration). The cost function can also be modified to align more closely with different association perspectives.

The resulting claim–storm associations reveal coherent spatial structures and a strong correlation between local wind gust intensity and damage, validating the physical basis of the approach. The 40 most damaging events identified from 1998 match well with existing storm databases, and cost metrics per storm align with previous findings from the insurance literature (Frédération France Assureur, 2025; Mission Risques Naturels, 2021). This highlights the method's robustness and its potential for systematic storm impact identification.

This paper investigated the impact of clusters of storms using ERA5 data, which can be a limitation when focusing on historical storm events. Discrepancies between reanalysis and observational datasets in terms of wind gust values are well documented (Flynn et al., 2024). The proposed method is based not only on the date of the storm but also on the wind-gust value observed at the claim location. It can thus be expected that with different meteorological input data, different impacting storms and consequently clusters could be identified. Exploring the sensitivity of outcomes to different meteorological sources would be a valuable step in testing the method's robustness.

Although assumptions were necessary to attribute claims to storms, direct attribution remains inherently uncertain. In particular, it was assumed that the damage resulted from the storm associated with the highest wind gust. The whole method was built to overcome the issue of not knowing the driver of the loss. As windgust is known to be one of the primary drivers of damage, this variable was used to disaggregate claims associated with overlapping events. Incorporating alternative variables, such as sustained 10m wind or upper-level wind, could lead to the detection of different impacting storms. However, recent research shows that claim behaviour aligns similarly with various wind metrics (Fonseca Cerda et al., 2024). In the context of storm clustering, attributing damage to a single event becomes especially challenging, as multiple storms with high wind intensity are observed at the same moment. Overlapping storms with high wind intensities often act collectively, and damage may arise from the persistent impact of several storms in quick succession. Because wind gusts are relatively localised, the method can distinguish between storm events when high-intensity winds occur in distinct areas (e.g., Storm Klaus Sect.4.2). Conversely, in cases like Lothar and Martin (Sect. 4.1), where the same locations experienced high wind gusts from multiple events, further analysis is required to compare the observed damage with what would be expected if each storm came outside of a cluster.

Clusters of storms were defined from an impact-centric perspective, using Generali's claim data. The choice of a 96h window reflects Generali's reinsurance aggregation policy, but this duration could be adjusted depending on in-place reinsurance policies. Larger aggregation windows could amplify clustering effects. While statistical metrics such as event dispersion could also define clusters, they do not easily support event-based attribution as required by impact modelling.

Accurate attribution has direct implications for reinsurance. Most contracts aggregate losses within a fixed time window, typically $72\mathrm{h}$ hours, but extended to $96\mathrm{h}$ hours in Generali's case. As the time window increases, closely spaced events are more likely to be grouped, reducing the number of reimbursable events and leading to lower overall reinsurance costs. Modifying this window can affect loss estimates and the financial response of reinsurers. We also observed that claims are sometimes reported up to three days before or after the actual storm date. Reassigning these claims to the appropriate storm would allow for a broader temporal grouping of losses. In practice, a $96\mathrm{h}$ reinsurance window could then encompass claims occurring over a total span of up to $240\mathrm{h}$.

Understanding historical storm clustering and comparing these patterns to those simulated in catastrophe models is essential for refining reinsurance structures and improving financial preparedness (Kaas, 2009; Khare et al., 2015). Clustering also raises questions about evolving vulnerability. Current catastrophe models often assume static vulnerability, failing to account for changing exposure or structural fatigue due to successive events. For instance, a building weakened by one storm might be more susceptible to damage from a subsequent event. Most vulnerability functions developed in the literature assume event independence (Dorland et al., 1999; Klawa and Ulbrich, 2003; Heneka et al., 2006; Schwierz et al., 2010; Prahl et al., 2015; Pardowitz et al., 2016). These assumptions should be critically revisited to assess how vulnerability evolves under compound stress. The correct attribution of losses, as proposed in this paper, is an important step toward building more dynamic vulnerability curves. Precise knowledge of the physical conditions leading to loss is essential to disentangle meteorological drivers from structural susceptibility. Future research could investigate whether the same building characteristics are consistently vulnerable during storm clusters or whether these features exhibit context-dependent behaviour.

A key strength of this work is its capacity to disentangle and attribute damage within storm clusters. Case studies, including storms Anatol, Lothar and Martin (Sect4.1), as well as storm Klaus (Sect4.2), demonstrate how simple date-based attribution is insufficient to isolate the impact of temporally or spatially overlapping events. Our study reveals that the most damaging storms are frequently part of storm clusters, confirming earlier work by Vitolo et al. (2009), which highlighted the tendency of intense ETCs to occur in series. This analysis further shows that the total loss associated with a cluster event is distributed across multiple storm members. This highlights the risk posed by storm clustering, where the overall damage arises from the combined effects of several interconnected storms, rather than being attributable to a single event.

6 Conclusions

The association method presented here offers a framework for improving our understanding of storm-related damage. We underline that a temporal window of a few days before and after, as well as a threshold over the minimal number of claims per event, was essential to capture all the impact. This method enhances the attribution of damage to specific physical events, which is key for risk assessment, loss estimation and prevention strategies. It also supports the identification of storm clusters and provides a foundation for assessing compounded risk. The study underlines an exacerbated impact linked to clusters of storms, which are responsible for 85% of the total losses since 1999 for Generali. We also showed that storms associated with damage exhibit more clustering than the set of potential ETCs impacting France. Within these clusters, the percentage of the

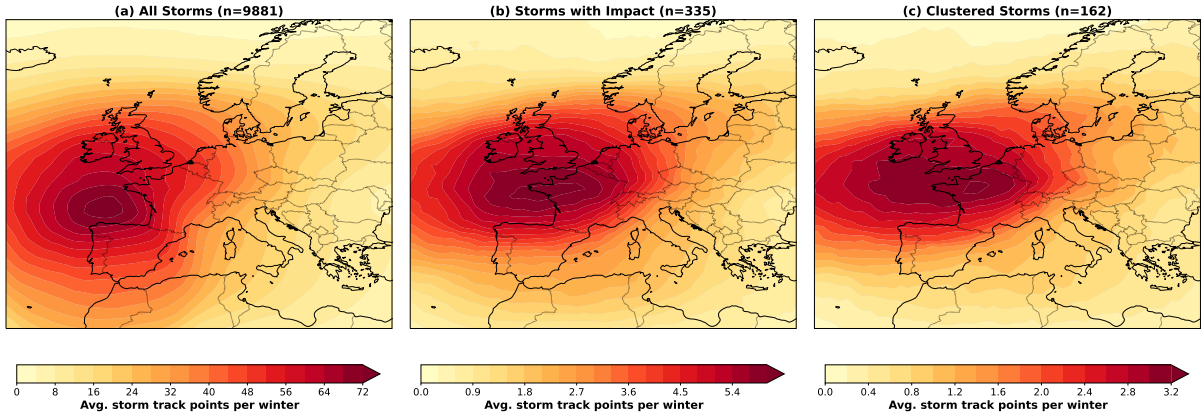

Figure A1. Distribution of storm tracks with an impact radius of $1300\mathrm{km}$ for the set of all storms (a), storms resulting in some impact for Generali (b) and storms resulting in a clustered impact (c)

loss held by the most costly storm varies widely, with an average contribution of 70% of total losses. Notably, this share is not influenced by the storm order of arrival. Case studies of well-known high-impact storms further validated the method's ability to disentangle the damages caused by successive storms. Overall, these results contribute to a more comprehensive understanding of how the interaction between hazard characteristics and exposure dynamics contributes to storm-related losses, supporting the development of more nuanced approaches for managing compound weather risks.

Appendix A: Storm track data

Appendix B: Sensitivity test with varying radius

The outcome of the association procedure depends on the definition of storm footprints and is therefore influenced by both the tracking algorithm and the definition of storm impact area. In this study, we adopted a broad characterisation of ETC, encompassing short-lived and localised depressions. Moreover, no distinction among depressions was made when constructing the storm footprints: a uniform radius of $1300\,\mathrm{km}$ was applied to all ETC throughout their entire life cycle. Since this choice can strongly affect the association between storm events and insurance claims, we tested alternative footprint definitions. Specifically, we reduced the constant radius to 1100 and $900\,\mathrm{km}$, and we further implemented a variable-radius approach conditioned on storm intensity, represented by the minimum sea-level pressure ($mslp$) observed during the cyclone's life cycle. In this latter case, the radius was defined as follows:

$$r = \begin{cases} 1300\,\mathrm{km}, & \text{if } mslp \leq 980\,\mathrm{hPa}, \\ 1100\,\mathrm{km}, & \text{if } 980 < mslp \leq 1000\,\mathrm{hPa}, \\ 900\,\mathrm{km}, & \text{if } mslp > 1000\,\mathrm{hPa}. \end{cases}$$

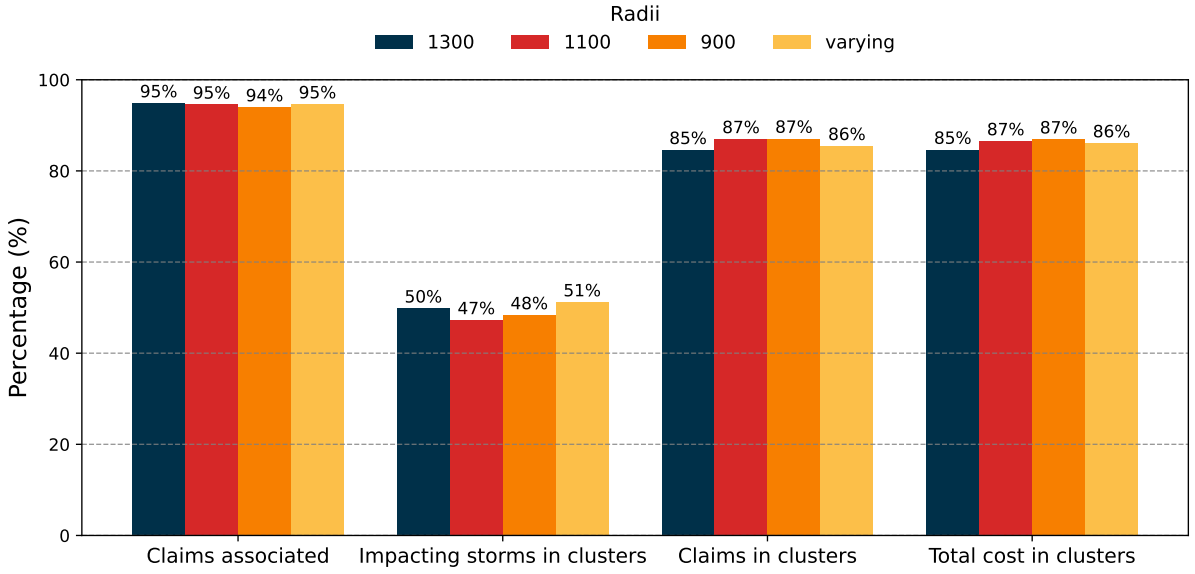

Figure B1. Percentage of claims from the raw data associated with a storm event, of storms in clusters, claims in clusters and the total cost associated with cluster events. Dark blue bars are the results of the associated used in the paper, red, orange and yellow bars are the results of perturbed associated performed using a radius of, respectively, $1100\mathrm{km}$, $900\mathrm{km}$ and a varying radius.

Using these alternative footprint definitions, the number of storms associated with impact was 332, 339, and 330 for the $1100\,\mathrm{km}$, $900\,\mathrm{km}$, and variable-radius cases, respectively. Figure B1 shows the corresponding results across several statistical indicators. Overall, the total number of claims associated with storms remained unchanged across the different configurations. Among storms linked to impacts, the proportion of those forming clusters is similar, ranging from 47% with the $1100\,\mathrm{km}$ radius to 51% with the variable radius. Likewise, both the number of claims and the total losses attributed to clustered storms remain of comparable magnitude regardless of the radius specification.

Appendix C: Sensitivity of the cost function

The cost function f_{cost} defined in Sect.3.2 varies as a function of the weight assigned to the frequency metric (w_{freq}). Fig. C1 shows the optimal values of the parameters X_b, X_a and n_{claims} as a function of the varying weight. It can be underlined that the optimal values of all the parameters are identical for the weight varying between 0.3 and 0.6. This means that, with a balanced penalty between the precision and frequency metrics, the optimal parameters are identical.

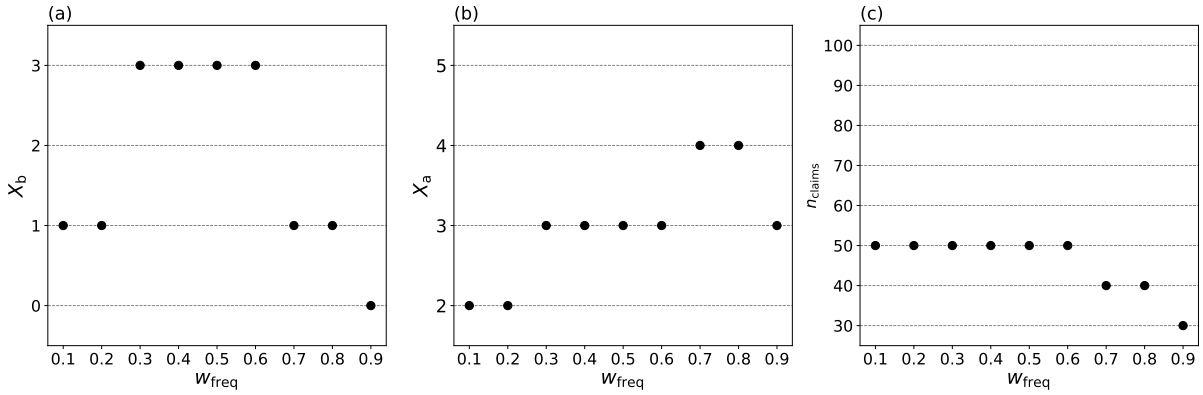

Figure C1. Optimal value of X_b (a), X_a (b) and n_{claims} (c) as a function of the weight of the frequency metric w_{freq}

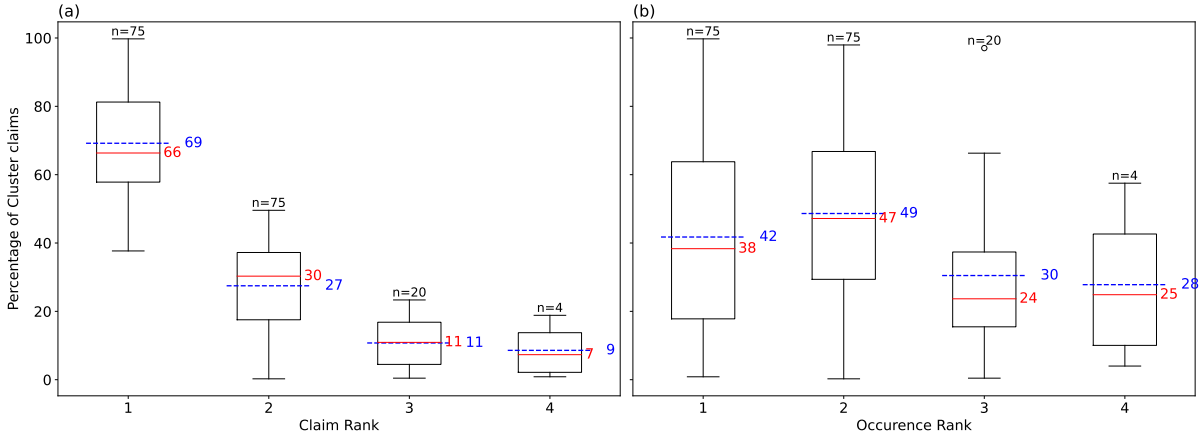

Figure D1. Distribution of the number of claims within the members of the cluster as a function of the claim rank (a) and occurrence rank (b). Thick red lines indicate the median, and blue dashed ones the mean. The numbers above each box correspond to the number of members used for each box plot.

Appendix D: Distribution of claim intensity within clusters

Fig. D1 shows the share of the claim intensity as a function of the claim and occurrence rank. A claims rank of 1 corresponds to the member of the cluster with the most number of claims.

Code availability. Scripts to reproduce the main results of this publication are available a thttps://doi.org/10.5281/zenodo.15771837 (Hasbini, 2025)

Data availability. ETC tracks were provided by Matthew Priestley. ERA5 data is openly available in Copernicus Climate Change Service Climate Data Store at https://doi.org/10.24381/cds.bd0915c6. Generali claims datasets analysed in the current study are not publicly available as they are proprietary to the company.

Author contributions. LH, PY, LB and AP conceptualised the experiments. LH produced the numerical experiments and analyses. LH and PY contributed to writing the paper.

Competing interests. The contact author has declared that neither of the authors has any competing interests. Authors LH, LB and AP are employed by Generali France.

Acknowledgements. This work was supported by the French ANRT, which funded LH's PhD thesis. We thank Matthew Priestley (U Exeter, UK) for useful discussions on the storm tracking algorithm. We also thank Quentin Henaff (Generali France) for valuable insights into the insurance claims and for maintaining the claim database.

References

AIR: Winter Storm Klaus: Findings From the AIR damage Survey, https://www.air-worldwide.com/Publications/AIR-Currents/attachments/AIR-Currents--Klaus/, accessed: 2025-02-19, 2009.

Base Adresse Nationale: Base Adresse Nationale (BAN), https://www.data.gouv.fr/datasets/base-adresse-nationale/informations, dataset available on data.gouv.fr, 2025.

Birkmann, J., Cardona, O. D., Carreño, M. L., Barbat, A. H., Pelling, M., Schneiderbauer, S., Kienberger, S., Keiler, M., Alexander, D., Zeil, P., and Welle, T.: Framing vulnerability, risk and societal responses: the MOVE framework, Natural Hazards, 67, 193–211, https://doi.org/10.1007/s11069-013-0558-5, 2013.

Bjerknes, J. and Solberg, H.: Life cycle of cyclones and the polar front theory of atmospheric circulation, vol. 3, Grondahl, 1922.

Bründl, M. and Rickli, C.: The storm Lothar 1999 in Switzerland–an incident analysis, Forest Snow and Landscape Research, 77, 207–216, 2002.

Copernicus C3S: Windstorm tracks and footprints derived from reanalysis over Europe between 1940 to present, https://doi.org/10.24381/BF1F06A9, 2025.

Copernicus Climate Change Service: Winter windstorm indicators for Europe from 1979 to 2021 derived from reanalysis, https://doi.org/10.24381/CDS.9B4EA013, 2020.

Cornér, J. S., Bouvier, C. G. F., Doiteau, B., Pantillon, F., and Sinclair, V. A.: Classification of North Atlantic and European extratropical cyclones using multiple measures of intensity, https://doi.org/10.5194/egusphere-2024-1749, 2024.

Dacre, H. F. and Pinto, J. G.: Serial clustering of extratropical cyclones: a review of where, when and why it occurs, npj Climate and Atmospheric Science, 3, 48, https://doi.org/10.1038/s41612-020-00152-9, 2020.

Dorland, C., Tol, R. S. J., and Palutikof, J. P.: Vulnerability of the Netherlands and Northwest Europe to Storm Damage under Climate Change, Climatic Change, 43, 513–535, https://doi.org/10.1023/A:1005492126814, 1999.

ECMWF: Insurance impacts of European windstorms, https://stories.ecmwf.int/insurance-impacts-of-european-windstorms/index.html, accessed: 2025-02-13, 2024.

Economou, T., Stephenson, D. B., Pinto, J. G., Shaffrey, L. C., and Zappa, G.: Serial clustering of extratropical cyclones in a multi-model ensemble of historical and future simulations, Quarterly Journal of the Royal Meteorological Society, 141, 3076–3087, https://doi.org/10.1002/qj.2591, 2015.

ESRI: Geocode Addresses (Geocoding), https://pro.arcgis.com/en/pro-app/latest/tool-reference/geocoding/geocode-addresses.htm, 2025.

Feser, F., Barcikowska, M., Krueger, O., Schenk, F., Weisse, R., and Xia, L.: Storminess over the North Atlantic and northwestern Europe—A review, Quarterly Journal of the Royal Meteorological Society, 141, 350–382, https://doi.org/10.1002/qj.2364, 2015.

Flaounas, E., Aragão, L., Bernini, L., Dafis, S., Doiteau, B., Flocas, H., Gray, S. L., Karwat, A., Kouroutzoglou, J., Lionello, P., Miglietta, M. M., Pantillon, F., Pasquero, C., Patlakas, P., Picornell, M. , Porcù, F., Priestley, M. D. K., Reale, M., Roberts, M. J., Saaroni, H., Sandler, D., Scoccimarro, E., Sprenger, M., and Ziv, B.: A composite approach to produce reference datasets for extratropical cyclone tracks: application to Mediterranean cyclones, Weather and Climate Dynamics, 4, 639–661, https://doi.org/10.5194/wcd-4-639-2023, 2023.

Flynn, C. M., Moemken, J., Pinto, J. G., and Messori, G.: A New Database of Extreme European Winter Windstorms, https://doi.org/10.5194/essd-2024-298, 2024.

Fonseca Cerda, M. D. S., De Moel, H., Van Ederen, D., Aerts, J. C. J. H., Botzen, W. J. W., and Haer, T.: Empirical evaluation of windstorm losses and meteorological variables over the Netherlands, Natural Hazards, https://doi.org/10.1007/s11069-024-07024-y, 2024.

Frédération France Assureur: L'assurance des évènements naturels en 2023, https://www.franceassureurs.fr/nos-chiffres-cles/assurance-de-dommages-et-responsabilite/lassurance-des-evenements-naturels-en-2023/, 2025.

Frédération France Assureurs: L'assurance habitation en 2023, https://www.franceassureurs.fr/nos-chiffres-cles/assurance-de-dommages-et-responsabilite/lassurance-habitation-en-2023/, 2024a.

Frédération France Assureurs: L'assurance de dommages aux biens des professionnels en 2023, https://www.franceassureurs.fr/nos-chiffres-cles/assurance-de-dommages-et-responsabilite/lassurance-habitation-en-2023/, 2024b.

Ginesta, M., Yiou, P., Messori, G., and Faranda, D.: A methodology for attributing severe extratropical cyclones to climate change based on reanalysis data: the case study of storm Alex 2020, Climate Dynamics, 61, 229–253, https://doi.org/10.1007/s00382-022-06565-x, 2023.

Gramcianinov, C., Campos, R., De Camargo, R., Hodges, K., Guedes Soares, C., and Da Silva Dias, P.: Analysis of Atlantic extratropical storm tracks characteristics in 41 years of ERA5 and CFSR/CFSv2 databases, Ocean Engineering, 216, 108 111, https://doi.org/10.1016/j.oceaneng.2020.108111, 2020.

Hasbini, L.: Unravelling the wind impact of clusters of storms, a case study over the French insurer Generali - Scripts, https://doi.org/10.5281/zenodo.15771837, 2025.

Hauser, S., Mueller, S., Chen, X., Chen, T., Pinto, J. G., and Grams, C. M.: The Linkage of Serial Cyclone Clustering in Western Europe and Weather Regimes in the North Atlantic-European Region in Boreal Winter, Geophysical Research Letters, 50, e2022GL101 900, https://doi.org/10.1029/2022GL101900, 2023.

Hawcroft, M., Walsh, E., Hodges, K., and Zappa, G.: Significantly increased extreme precipitation expected in Europe and North America from extratropical cyclones, Environmental Research Letters, 13, 124 006, https://doi.org/10.1088/1748-9326/aaed59, 2018.

Hawcroft, M. K., Shaffrey, L. C., Hodges, K. I., and Dacre, H. F.: How much Northern Hemisphere precipitation is associated with extratropical cyclones?, Geophysical Research Letters, 39, 2012GL053 866, https://doi.org/10.1029/2012GL053866, 2012.

Heneka, P., Hofherr, T., Ruck, B., and Kottmeier, C.: Winter storm risk of residential structures – model development and application to the German state of Baden-Württemberg, Natural Hazards and Earth System Sciences, 6, 721–733, https://doi.org/10.5194/nhess-6-721-2006, 2006.

Hersbach, H., Bell, B., Berrisford, P., Hirahara, S., Horányi, A., Muñoz-Sabater, J., Nicolas, J., Peubey, C., Radu, R., Schepers, D., Simmons, A., Soci, C., Abdalla, S., Abellan, X., Balsamo, G., Bechtold, P., Biavati, G., Bidlot, J., Bonavita, M., De Chiara, G., Dahlgren, P., Dee, D., Diamantakis, M., Dragani, R., Flemming, J., Forbes, R., Fuentes, M., Geer, A., Haimberger, L., Healy, S., Hogan, R. J., Hólm, E., Janisková, M., Keeley, S., Laloyaux, P., Lopez, P., Lupu, C., Radnoti, G., De Rosnay, P., Rozum, I., Vamborg, F., Villaume, S., and Thépaut, J.: The ERA5 global reanalysis, Quarterly Journal of the Royal Meteorological Society, 146, 1999–2049, https://doi.org/10.1002/qj.3803, 2020.

Hillier, J. K., Bloomfield, H. C., Manning, C., Garry, F., Shaffrey, L., Bates, P., and Kumar, D.: Increasingly Seasonal Jet Stream Raises Risk of Co-Occurring Flooding and Extreme Wind in Great Britain, International Journal of Climatology, 45, e8763, https://doi.org/10.1002/joc.8763, 2025.

Hodges, K. I.: Adaptive Constraints for Feature Tracking, Monthly Weather Review, 127, 1362–1373, https://doi.org/10.1175/1520-0493(1999)127<1362:ACFFT>2.0.CO;2, 1999.

INSEE: Coefficient de transformation de l'euro ou du franc d'une année, en euro ou en franc d'une autre année – Base 2015, https://www.insee.fr/fr/statistiques/serie/010605954, 2025.

Intergovernmental Panel On Climate Change: Climate Change 2021 – The Physical Science Basis: Working Group I Contribution to the Sixth Assessment Report of the Intergovernmental Panel on Climate Change, Cambridge University Press, 1 edn., https://doi.org/10.1017/9781009157896, 2023.

Kaas, R.: Modern actuarial risk theory: using R, Springer, Berlin [New York], 2nd ed edn., 2009.

Karwat, A., Franzke, C. L. E., Pinto, J. G., Lee, S.-S., and Blender, R.: Northern Hemisphere Extra-Tropical Cyclone Clustering in ERA5 Reanalysis and the CESM2 Large Ensemble, Journal of Climate, https://doi.org/10.1175/JCLI-D-23-0160.1, 2023.

Kettle, A. J.: Storm Anatol over Europe in December 1999: impacts on societal and energy infrastructure, Advances in Geosciences, 56, 141–153, https://doi.org/10.5194/adgeo-56-141-2021, 2021.

Khare, S., Bonazzi, A., Mitas, C., and Jewson, S.: Modelling clustering of natural hazard phenomena and the effect on re/insurance loss perspectives, Natural Hazards and Earth System Sciences, 15, 1357–1370, https://doi.org/10.5194/nhess-15-1357-2015, 2015.

Klawa, M. and Ulbrich, U.: A model for the estimation of storm losses and the identification of severe winter storms in Germany, Natural Hazards and Earth System Sciences, 3, 725–732, https://doi.org/10.5194/nhess-3-725-2003, 2003.

Kron, W., Steuer, M., Löw, P., and Wirtz, A.: How to deal properly with a natural catastrophe database – analysis of flood losses, Natural Hazards and Earth System Sciences, 12, 535–550, https://doi.org/10.5194/nhess-12-535-2012, 2012.

Leckebusch, G. C., Renggli, D., and Ulbrich, U.: Development and application of an objective storm severity measure for the Northeast Atlantic region, Meteorologische Zeitschrift, 17, 575–587, https://doi.org/10.1127/0941-2948/2008/0323, 2008.

Liberato, M. L. R., Pinto, J. G., Trigo, I. F., and Trigo, R. M.: Klaus – an exceptional winter storm over northern Iberia and southern France, Weather, 66, 330–334, https://doi.org/10.1002/wea.755, 2011.

Little, A. S., Priestley, M. D. K., and Catto, J. L.: Future increased risk from extratropical windstorms in northern Europe, Nature Communications, 14, 4434, https://doi.org/10.1038/s41467-023-40102-6, 2023.

Lockwood, J. F., Guentchev, G. S., Alabaster, A., Brown, S. J., Palin, E. J., Roberts, M. J., and Thornton, H. E.: Using high-resolution global climate models from the PRIMAVERA project to create a European winter windstorm event set, Natural Hazards and Earth System Sciences, 22, 3585–3606, https://doi.org/10.5194/nhess-22-3585-2022, 2022.

Ludwig, P., Pinto, J. G., Hoepp, S. A., Fink, A. H., and Gray, S. L.: Secondary Cyclogenesis along an Occluded Front Leading to Damaging Wind Gusts: Windstorm Kyrill, January 2007, Monthly Weather Review, 143, 1417–1437, https://doi.org/10.1175/MWR-D-14-00304.1, 2015.

Mailier, P. J., Stephenson, D. B., Ferro, C. A. T., and Hodges, K. I.: Serial Clustering of Extratropical Cyclones, Monthly Weather Review, 134, 2224–2240, https://doi.org/10.1175/MWR3160.1, 2006.

Meteo France: Tempêtes et changement climatique, https://meteofrance.com/changement-climatique/observer/tempetes-et-changement-climatique, 2023.

Michèle Lai: Twenty years after storms Anatol, Lothar and Martin: Memories from the end of the millennium, https://www.moodys.com/web/en/us/insights/insurance/twenty-years-after-storms-anatol-lothar-and-martin-memories-from-the-end-of-the-millennium.html, accessed: 2025-02-19, 2019.

Mission Risques Naturels: Lettre d'information de la mission risques naturels 36, https://www.mrn.asso.fr/wp-content/uploads/2021/07/lettre-n36_vf.pdf, 2021.

Moemken, J., Alifdini, I., Ramos, A. M., Georgiadis, A., Brocklehurst, A., Braun, L., and Pinto, J. G.: Insurance loss model vs meteorological loss index – How comparable are their loss estimates for European windstorms?, preprint, Atmospheric, Meteorological and Climatological Hazards, https://doi.org/10.5194/nhess-2024-16, 2024a.

Moemken, J., Messori, G., and Pinto, J. G.: Windstorm losses in Europe – What to gain from damage datasets, Weather and Climate Extremes, 44, 100 661, https://doi.org/10.1016/j.wace.2024.100661, 2024b.

Munich RE: Data on natural disasters since 1980 - Munich Re's NatCatSERVICE, https://www.munichre.com/en/solutions/for-industry-clients/natcatservice.html, accessed: 2025-02-20, 2025.

Neu, U., Akperov, M. G., Bellenbaum, N., Benestad, R., Blender, R., Caballero, R., Cocozza, A., Dacre, H. F., Feng, Y., Fraedrich, K., Grieger, J., Gulev, S., Hanley, J., Hewson, T., Inatsu, M., Keay, K., Kew, S. F., Kindem, I., Leckebusch, G. C., Liberato, M. L. R., Lionello, P., Mokhov, I. I., Pinto, J. G., Raible, C. C., Reale, M., Rudeva, I., Schuster, M., Simmonds, I., Sinclair, M., Sprenger, M., Tilinina, N. D., Trigo, I. F., Ulbrich, S., Ulbrich, U., Wang, X. L., and Wernli, H.: IMILAST: A Community Effort to Intercompare Extratropical Cyclone Detection and Tracking Algorithms, Bulletin of the American Meteorological Society, 94, 529–547, https://doi.org/10.1175/BAMS-D-11-00154.1, 2013.

Pardowitz, T., Osinski, R., Kruschke, T., and Ulbrich, U.: An analysis of uncertainties and skill in forecasts of winter storm losses, Natural Hazards and Earth System Sciences, 16, 2391–2402, https://doi.org/10.5194/nhess-16-2391-2016, 2016.

PERILS: Event loss information, https://www.perils.org/losses?year=&classification=1012&status=#event-losses, accessed: 2025-02-20, 2025.

Pinto, J. G., Gómara, I., Masato, G., Dacre, H. F., Woollings, T., and Caballero, R.: Large-scale dynamics associated with clustering of extratropical cyclones affecting Western Europe, Journal of Geophysical Research: Atmospheres, 119, https://doi.org/10.1002/2014JD022305, 2014.

Pinto, J. G., Ulbrich, S., Economou, T., Stephenson, D. B., Karremann, M. K., and Shaffrey, L. C.: Robustness of serial clustering of extratropical cyclones to the choice of tracking method, Tellus A: Dynamic Meteorology and Oceanography, 68, 32 204, https://doi.org/10.3402/tellusa.v68.32204, 2016.

Prahl, B. F., Rybski, D., Burghoff, O., and Kropp, J. P.: Comparison of storm damage functions and their performance, Natural Hazards and Earth System Sciences, 15, 769–788, https://doi.org/10.5194/nhess-15-769-2015, 2015.

Priestley, M. D. K., Pinto, J. G., Dacre, H. F., and Shaffrey, L. C.: The role of cyclone clustering during the stormy winter of 2013/2014, Weather, 72, 187–192, https://doi.org/10.1002/wea.3025, 2017a.

Priestley, M. D. K., Pinto, J. G., Dacre, H. F., and Shaffrey, L. C.: Rossby wave breaking, the upper level jet, and serial clustering of extratropical cyclones in western Europe, Geophysical Research Letters, 44, 514–521, https://doi.org/10.1002/2016GL071277, 2017b.

Priestley, M. D. K., Dacre, H. F., Shaffrey, L. C., Schemm, S., and Pinto, J. G.: The role of secondary cyclones and cyclone families for the North Atlantic storm track and clustering over western Europe, Quarterly Journal of the Royal Meteorological Society, 146, 1184–1205, https://doi.org/10.1002/qj.3733, 2020.

Priestley, M. D. K., Stephenson, D. B., Scaife, A. A., Bannister, D., Allen, C. J. T., and Wilkie, D.: Return levels of extreme European windstorms, their dependency on the North Atlantic Oscillation, and potential future risks, Natural Hazards and Earth System Sciences, 23, 3845–3861, https://doi.org/10.5194/nhess-23-3845-2023, 2023.

Priestley, M. D. K., Stephenson, D. B., Scaife, A. A., Bannister, D., Allen, C. J. T., and Wilkie, D.: Forced trends and internal variability in climate change projections of extreme European windstorm frequency and severity, Quarterly Journal of the Royal Meteorological Society, 150, 4933–4950, https://doi.org/10.1002/qj.4849, 2024.

Raible, C. C., Della-Marta, P. M., Schwierz, C., Wernli, H., and Blender, R.: Northern Hemisphere Extratropical Cyclones: A Comparison of Detection and Tracking Methods and Different Reanalyses, Monthly Weather Review, 136, 880–897, https://doi.org/10.1175/2007MWR2143.1, 2008.

Risk Management Solutions, Inc: Windstorms Lothar and Martin, https://forms2.rms.com/rs/729-DJX-565/images/ws_1999_windstorms_lothar_martin.pdf, accessed: 2025-02-19, 2000.

Rivière, G., Arbogast, P., Maynard, K., and Joly, A.: The essential ingredients leading to the explosive growth stage of the European wind storm *Lothar* of Christmas 1999, Quarterly Journal of the Royal Meteorological Society, 136, 638–652, https://doi.org/10.1002/qj.585, 2010.

Roberts, J. F., Champion, A. J., Dawkins, L. C., Hodges, K. I., Shaffrey, L. C., Stephenson, D. B., Stringer, M. A., Thornton, H. E., and Youngman, B. D.: The XWS open access catalogue of extreme European windstorms from 1979 to 2012, Natural Hazards and Earth System Sciences, 14, 2487–2501, https://doi.org/10.5194/nhess-14-2487-2014, 2014.

Schindler, D., Grebhan, K., Albrecht, A., and Schönborn, J.: Modelling the wind damage probability in forests in Southwestern Germany for the 1999 winter storm 'Lothar', International Journal of Biometeorology, 53, 543–554, https://doi.org/10.1007/s00484-009-0242-3, 2009.

Schmoeckel, J. and Kottmeier, C.: Storm damage in the Black Forest caused by the winter storm "Lothar" – Part 1: Airborne damage assessment, Natural Hazards and Earth System Sciences, 8, 795–803, https://doi.org/10.5194/nhess-8-795-2008, 2008.

Schwierz, C., Köllner-Heck, P., Zenklusen Mutter, E., Bresch, D. N., Vidale, P.-L., Wild, M., and Schär, C.: Modelling European winter wind storm losses in current and future climate, Climatic Change, 101, 485–514, https://doi.org/10.1007/s10584-009-9712-1, 2010.

Severino, L. G., Kropf, C. M., Afargan-Gerstman, H., Fairless, C., De Vries, A. J., Domeisen, D. I. V., and Bresch, D. N.: Projections and uncertainties of winter windstorm damage in Europe in a changing climate, Natural Hazards and Earth System Sciences, 24, 1555–1578, https://doi.org/10.5194/nhess-24-1555-2024, 2024.

Sinclair, V. A. and Catto, J. L.: The relationship between extra-tropical cyclone intensity and precipitation in idealised current and future climates, Weather and Climate Dynamics, 4, 567–589, https://doi.org/10.5194/wcd-4-567-2023, 2023.

Stucki, P., Brönnimann, S., Martius, O., Welker, C., Imhof, M., Von Wattenwyl, N., and Philipp, N.: A catalog of high-impact windstorms in Switzerland since 1859, Natural Hazards and Earth System Sciences, 14, 2867–2882, https://doi.org/10.5194/nhess-14-2867-2014, 2014.

Vitolo, R., Stephenson, D. B., Cook, I. M., and Mitchell-Wallace, K.: Serial clustering of intense European storms, Meteorologische Zeitschrift, 18, 411–424, https://doi.org/10.1127/0941-2948/2009/0393, 2009.

Welker, C., Röösli, T., and Bresch, D. N.: Comparing an insurer's perspective on building damages with modelled damages from pan-European winter windstorm event sets: a case study from Zurich, Switzerland, Natural Hazards and Earth System Sciences, 21, 279–299, https://doi.org/10.5194/nhess-21-279-2021, 2021.

Wernli, H., Dirren, S., Liniger, M. A., and Zillig, M.: Dynamical aspects of the life cycle of the winter storm 'Lothar' (24–26 December 1999), Quarterly Journal of the Royal Meteorological Society, 128, 405–429, https://doi.org/10.1256/003590002321042036, 2002.

Zappa, G., Shaffrey, L. C., and Hodges, K. I.: The Ability of CMIP5 Models to Simulate North Atlantic Extratropical Cyclones*, Journal of Climate, 26, 5379–5396, https://doi.org/10.1175/JCLI-D-12-00501.1, 2013.